

Copyright

by

Abdulaziz Samir Altubayyeb

2014

**The Thesis Committee for Abdulaziz Samir Altubayyeb
Certifies that this is the approved version of the following thesis:**

**A Numerical Study of the Impact of Waterflood Pattern Size on
Ultimate Recovery in Undersaturated Oil Reservoirs**

**APPROVED BY
SUPERVISING COMMITTEE:**

Supervisor:

Larry W. Lake

Mark W. McClure

**A Numerical Study of the Impact of Waterflood Pattern Size on
Ultimate Recovery in Undersaturated Oil Reservoirs**

by

Abdulaziz Samir Altubayyeb, B.S.

Thesis

Presented to the Faculty of the Graduate School of

The University of Texas at Austin

in Partial Fulfillment

of the Requirements

for the Degree of

Master of Science in Engineering

The University of Texas at Austin

August 2014

Dedication

To my mother, my father, my sisters, and my wife.

Acknowledgements

I would like to express my sincere gratitude to my research advisor Dr. Larry Lake for his continuous guidance and support throughout my time at the University of Texas at Austin. Working with him on this research has been a truly remarkable experience. I would like to acknowledge Dr. Mark McClure for his feedback on this thesis. I would also like to extend my thanks to all the faculty and staff at the Petroleum Engineering Department for creating such a positive learning environment. I would like to acknowledge the Computer Modeling Group (CMG) for developing the simulator used in this research. I would also like to thank my fellow graduate students Murtadha Al Tammar and Emad Alabbad for their support inside and outside the classroom. Many thanks also go to Lokendra Jain for all the help he provided me with CMG.

Special thanks are due to my sponsors at Saudi Aramco for presenting me with the opportunity of pursuing this graduate degree. I would like to acknowledge the members of the Khurais and Central Arabia Reservoir Management Team for all the knowledge they have passed on to me. My appreciation also goes to all the professors at the Colorado School of Mines Petroleum Engineering Department for the valuable undergraduate education they provided me with.

My deepest gratitude goes to my family for their continuous support, guidance and inspiration. I am indebted to my parents for everything they have ever done for me. Making them proud has always been my strongest motivator.

Abstract

A Numerical Study of the Impact of Waterflood Pattern Size on Ultimate Recovery in Undersaturated Oil Reservoirs

Abdulaziz Samir Altubayyeb, M.S.E.

The University of Texas at Austin, 2014

Supervisor: Larry W. Lake

The reserve growth potential of existing conventional oil reservoirs is huge. This research, through numerical simulation, aims to evaluate pattern size reduction as a strategy for improving waterflood recovery in undersaturated oil reservoirs.

A plethora of studies have reported improvements in waterflood recovery resulting from pattern size reduction in heterogeneous reservoirs. The dependence of waterflood recovery on pattern size was attributed to factors such as areal reservoir discontinuity, preferential flooding directions, “wedge-edge” oil recovery, irregular pattern geometry, communication with water-bearing zones, vertical reservoir discontinuity, and project economics (Driscoll, 1974). Though many of these publications relied on decline curve analysis in estimating ultimate oil recovery, simulations completed in this thesis support their findings, specifically for compartmentalized reservoirs, fractured reservoirs, and layered reservoirs.

Geostatistically-generated permeability fields were employed in the creation of various types of reservoir models. These models were populated with vertical production

and injection wells. Sensitivity analysis was then performed on three development scenarios: 160, 40, and 10 acre five-spots. Based on assigned production and injection constraints, the quantity of oil recovered at simulation termination was used to calculate ultimate recovery efficiency.

In homogeneous reservoir models, simulation results suggest that waterflood recovery was independent of pattern size. Similar results were also obtained from models with highly-variable non-zero permeabilities.

On the other hand, pattern size reduction was found to enhance oil recovery from reservoir models with a high degree of permeability anisotropy. In such reservoirs, recovery was found to be highly dependent on bottom-hole injection pressures. The higher the injection pressure the larger the quantity of oil bypassed by widely spaced patterns.

Likewise, high infill potential exists for reservoir models exhibiting areal discontinuity. In these types of models, the improvement in waterflood recovery resulting from pattern size reduction was directly related to the percentage of imbedded zero-permeability grid blocks. Ultimate oil recovery depended on the percolation of permeable grid blocks between production and injection wells.

Increasing well density also enhanced waterflood recovery in vertically discontinuous reservoir models. In such layered reservoirs, the amount oil unswept with large patterns was considerably diminished because of the improved injection profiles associated with tighter patterns.

Table of Contents

Table of Contents	viii
List of Tables	xi
List of Figures	xii
Chapter 1: Introduction	1
1.1 Motivation.....	1
1.2 Thesis Roadmap.....	2
Chapter 2: Engineered Waterdrive.....	3
2.1 History.....	3
2.2 Purpose.....	4
2.3 Water Injection Performance	4
2.3.1 Reservoir Properties.....	4
2.3.1.1 Heterogeneity.....	5
2.3.2 Fluid Properties	7
2.3.3 Development Strategies	8
2.3.3 Operation Strategies.....	12
Chapter 3: Literature Review.....	13
3.1 Field Performance Data	13
3.1.1 Little Buffalo Basin Field	13
3.1.2 Yates-Queen Sand.....	15
3.1.3 Grayburg Dolomite	16
3.1.4 Slaughter Field.....	17
3.1.5 Permian Basin Units	18
3.1.6 Means San Andres Unit	20
3.1.7 Fullerton Field.....	20
3.1.8 Robertson Field.....	21
3.1.9 IAB Field	21
3.1.10 Howard-Glasscock Field.....	21

3.1.11 Hewitt Field	22
3.1.12 Loudon Field	22
3.1.13 El Morgan Field	22
3.1.14 McElroy Field: Section 205	23
3.1.15 Prudhoe Bay Field.....	25
3.2 Rationale	27
3.2.1 Areal Reservoir Discontinuity	27
3.2.2 Preferential Flooding Directions.....	28
3.2.3 “Wedge-Edge” Oil Recovery.....	29
3.2.4 Irregular Pattern Geometry	30
3.2.5 Vertical Communication with Water-Bearing Zones	31
3.2.6 Layered Reservoirs	32
3.2.7 Project Economics	33
3.3 Summary	34
Chapter 4: Model Development.....	35
4.1 Grid Definition.....	35
4.2 Initial Conditions	36
4.3 PVT Properties.....	36
4.3 Flow Properties	37
4.4 Porosity and Permeability	38
4.5 Vertical Well Placement and Constraints	39
Chapter 5: Simulation Results and Discussion	42
5.1 Homogeneous Cases	42
5.1.1 Regular Patterns.....	42
5.1.2 Irregular Patterns.....	43
5.2 Heterogeneous Cases	45
5.2.1 Reservoirs with Highly-Variable Non-Zero Permeabilities	45
5.2.2 Reservoirs with Preferential Flooding Orientations	47
5.2.3 Areal Discontinuous Reservoirs	53
5.2.4 Layered Reservoirs	58

Chapter 6: Summary and Conclusion	67
6.1 Summary	67
6.2 Conclusion	69
References.....	71

List of Tables

Table 4.1: Fluid Properties.....	36
Table 4.2: The Development Scenarios Used in the Simulations.....	40
Table 5.1: Simulation Results for a 50 md Homogeneous Reservoir.....	42
Table 5.2: Simulation Results for Reservoirs with Highly-Variable Permeabilities and an Average Permeability of 50 md.	47
Table 5.3: Simulation Results for a Three-Dimensional Vertically Discontinuous Reservoir Model Reservoir (k_{avg} of Top Two Layers = 1 md, k_{avg} of Bottom Two Layers = 100 md).....	60
Table 5.4: Simulation Results for a Two-Dimensional Vertically Discontinuous Reservoir Model Reservoir (k_{avg} of Top Two Layers = 1 md, k_{avg} of Bottom Two Layers = 100 md).....	64

List of Figures

Figure 2.1: Mobile Oil Recovery as a Function of Reservoir Heterogeneity for Different Clastic Reservoirs (Fisher, 2013).	5
Figure 2.2: Stratigraphic Correlation Based on Better Understanding of Reservoir Geology (Fisher, 2013).	7
Figure 2.3: Peripheral Water Injection Examples (Craft and Hawkins, 1991).	9
Figure 2.4: Well Locations in Some Common Pattern Floods (Craft and Hawkins, 1991).	9
Figure 2.5: Field Performance of a Shallow Shelf Carbonate Reservoir (Fisher, 2013).	11
Figure 3.1: The Effect of Pattern Size Reduction on the Performance of Little Buffalo Basin's Tensleep Reservoir (Emmett et al., 1971).	14
Figure 3.2: Waterflood Response to Pattern Size Reduction Yates-Queen Sands (Driscoll, 1974).	15
Figure 3.3: The Impact of Decreasing Pattern Size on Oil Production from a Grayburg Dolomite Reservoir (Driscoll, 1974).	16
Figure 3.4: Waterflood Recovery as a Function of Well Spacing in Slaughter Field (van Everdingen, 1980).	17
Figure 3.5: Waterflood Recovery as a Function of Well Spacing for Permian Basin Units with Reservoir Permeability Ranging from 0.4 md to 0.8 md (Kern, 1981).	19
Figure 3.6: Waterflood Recovery as a Function of Well Spacing for Permian Basin Units with Reservoir Permeability Lower than 0.4 md (Kern, 1981).	19

Figure 3.7: The Impact of Pattern Realignment on Oil Production and Water Injection on Section 205 of the McElroy Field (Lemen, 1990).	25
Figure 3.8: The Effect of Well Spacing on Oil Recovery in the Prudhoe Bay Field (Kwan, 1992).	26
Figure 3.9: Reservoir Continuity as a Function of Horizontal Distance in the Wasson Sand Andres Field (Driscoll, 1974).	28
Figure 3.10: Five-Spot Waterflood with East-West Fracture Orientation (Driscoll, 1974).	29
Figure 3.11: Unswept Oil at the Edge of the Field (Driscoll, 1974).	29
Figure 3.12: The Improvement in Areal Sweep Achieved through Infill Drilling “Chickenwire” Patterns (Driscoll, 1974).	30
Figure 3.13: Vertical Communication with Water-Bearing Zones (Driscoll, 1974).	31
Figure 3.14: Vertically Discontinuous Pay Zones with (Driscoll, 1974).	32
Figure 3.15: The Effect of Formation Capacity on Economic Waterflood Recovery in the Levelland Unit (Driscoll, 1974).	33
Figure 4.1: Model Grid Top Depths.	35
Figure 4.2: Oil-Water Relative Permeability Curves.	37
Figure 4.3: Oil-Water Capillary Pressure as a Function of Water Saturation.	38
Figure 4.4: 160 Acre Five-Spot Development Scenario.	40
Figure 4.5: 40 Acre Five-Spot Development Scenario.	41
Figure 4.6: 10 Acre Five-Spot Development Scenario.	41
Figure 5.1: Cumulative Oil Production as a Function of Time for a 50 md Homogeneous Reservoir Developed with Five-Spot Patterns of Different Sizes.	43

Figure 5.2: Top View of a 10 md Homogeneous Three-Dimensional Reservoir Model Developed with Chickenwire Patterns.....	44
Figure 5.3: Top View of a 10 md Homogeneous Three-Dimensional Reservoir Model Developed with Chickenwire Patterns and Infill Wells.....	44
Figure 5.4: Permeability Distribution in a Spatially Uncorrelated Reservoir Model with an Average Permeability of 50 md.	45
Figure 5.5: Permeability Distribution in a Reservoir Model with an Average Permeability of 50 md and Autocorrelation Lengths of 7,472 ft in the x and y Directions.	46
Figure 5.6: Permeability Distribution in a Reservoir Model with an Average Permeability of 50 md and Autocorrelation Lengths of 7,472 ft in the x and z Directions.	46
Figure 5.7: Permeability in the x and z Directions for an Anisotropic Reservoir Model ($k_{avg} = 1,000$ md).....	48
Figure 5.8: Permeability in the y Direction for an Anisotropic Reservoir Model ($k_{avg} =$ 5 md).....	48
Figure 5.9: Recovery Efficiency as a Function of Bottom-Hole Injection Pressure for an Anisotropic Reservoir Model ($k_x/k_y=200$) Developed with Five-Spot Patterns of Different Sizes.	49
Figure 5.10: Oil Saturation at Simulation Termination for an Anisotropic Reservoir ($k_x/k_y=200$) Developed with 160 Acre Five-Spot Patterns (Bottom-Hole Injection Pressure = 5,000 psi).	50
Figure 5.11: Oil Saturation at Simulation Termination for an Anisotropic Reservoir ($k_x/k_y=200$) Developed with 40 Acre Five-Spot Patterns (Bottom-Hole Injection Pressure = 5,000 psi).	51

Figure 5.12: Oil Saturation at Simulation Termination for an Anisotropic Reservoir ($k_x/k_y=200$) Developed with 10 Acre Five-Spot Patterns (Bottom-Hole Injection Pressure = 5,000 psi).	51
Figure 5.13: Daily Oil Production Rate as a Function of Cumulative Oil Production for an Anisotropic Reservoir ($k_x/k_y=200$) Developed with Five-Spot Patterns of Different Sizes (Bottom-Hole Injection Pressure = 5,000 psi).	52
Figure 5.14: Recovery Efficiency as a Function of the Percentage of Non-Porous Impermeable Grid Blocks.	54
Figure 5.15: Permeability Distribution in a Spatially Uncorrelated Reservoir Model with 62.87% Non-Porous Impermeable Grid Blocks (Legend Colors in Logarithmic Scale).	55
Figure 5.16: Oil Saturation at Simulation Termination for an Areally Discontinuous Reservoir (62.87% Non-Porous Impermeable Grid Blocks) Developed with 160 Acre Five-Spot Patterns.	56
Figure 5.17: Oil Saturation at Simulation Termination for an Areally Discontinuous Reservoir (62.87% Non-Porous Impermeable Grid Blocks) Developed with 40 Acre Five-Spot Patterns.	56
Figure 5.18: Oil Saturation at Simulation Termination for an Areally Discontinuous Reservoir (62.87% Non-Porous Impermeable Grid Blocks) Developed with 10 Acre Five-Spot Patterns.	57
Figure 5.19: Daily Oil Production Rate as a Function of Cumulative Oil Production for an Areally Discontinuous Reservoir (62.87% Non-Porous Impermeable Grid Blocks).	57

Figure 5.20: Permeability Distribution for a Vertically Discontinuous Reservoir (k_{avg} of Top Two Layers = 1 md, k_{avg} of Bottom Two Layers = 100 md).	59
Figure 5.21: Oil Saturation at Simulation Termination for a Vertically Discontinuous Reservoir Developed with 160 Acre Five-Spots (k_{avg} of Top Two Layers = 1 md, k_{avg} of Bottom Two Layers = 100 md).	60
Figure 5.22: Oil Saturation at Simulation Termination for a Vertically Discontinuous Reservoir Developed with 40 Acre Five-Spots (k_{avg} of Top Two Layers = 1 md, k_{avg} of Bottom Two Layers = 100 md).	61
Figure 5.23: Oil Saturation at Simulation Termination for a Vertically Discontinuous Reservoir Developed with 10 Acre Five-Spots (k_{avg} of Top Two Layers = 1 md, k_{avg} of Bottom Two Layers = 100 md).	61
Figure 5.24: Cumulative Oil Production as a Function of Time for a Vertically Discontinuous Reservoir (k_{avg} of Top Two Layers = 1 md, k_{avg} of Bottom Two Layers = 100 md).	62
Figure 5.25: Permeability Distribution for a 2D Vertically Discontinuous Reservoir Model (k_{avg} of Top Two Layers = 1 md, k_{avg} of Bottom Two Layers = 100 md).	63
Figure 5.26: Oil Saturation at Simulation Termination for a 2D Vertically Discontinuous Reservoir Model Populated with wells that are 1,868 ft Apart.	64
Figure 5.27: Oil Saturation at Simulation Termination for a 2D Vertically Discontinuous Reservoir Model Populated with wells that are 934 ft Apart.	65

Figure 5.28: Oil Saturation at Simulation Termination for a 2D Vertically
Discontinuous Reservoir Model Populated with wells that are 467 ft
Apart.65

Figure 6.1: The Average Improvement in Ultimate Recovery Efficiency Achieved by
Reducing the Pattern Size from 160 to 10 Acre Five-Spots for all the
Performed Simulations.....67

Chapter 1: Introduction

1.1 MOTIVATION

Over 2 trillion barrels of oil have been added to the world's proven oil reserves in the last 30 years. 70% of these additional reserves have come from existing fields through better reservoir understanding and optimized development strategies. In fact, for conventional reservoirs, the potential of adding oil reserves from existing fields surpasses that of new field discovery (Fisher, 2013).

In terms of development strategies, waterflooding is considered the cheapest and most popular fluid injection recovery method. Water injection is implemented to improve productivity by maintaining reservoir pressure (or restoring pressure in depleted reservoirs) and by sweeping oil towards the production wells. Based on reservoir attributes, production and injection wells can be configured in different patterns: peripheral patterns, regular patterns, or irregular patterns. The size of these patterns has the potential of influencing waterflood performance.

In recent decades, the effect of pattern size on waterflood recovery has been widely disputed. Prior to 1960, a common belief was that no relationship existed between well spacing and hydrocarbon recovery (Wu et al., 1989). Since then, a plethora of studies have used field performance data to argue that waterflood recovery increases with increasing well density in heterogeneous reservoirs. However, most of these reports relied on decline curve analysis to estimate ultimate recovery. This study, through numerical simulation, aims to evaluate the impact of pattern size on waterflood recovery in different types of oil reservoirs.

1.2 THESIS ROADMAP

The upcoming chapters of this thesis follow the main themes addressed in the previous motivation section: waterflooding, reservoir heterogeneity, pattern size, and waterflood recovery. Chapter 2 reviews the main concepts of waterflooding operations. It starts off with a brief history of water injection followed by the purpose of such operations. It then moves on to discuss the main factors that influence waterflood performance including reservoir and fluid properties. The chapter then concludes with some notes on well placement. Chapter 3 reviews the literature pertaining to the effect of pattern size on waterflood recovery. It does so by presenting the response of different reservoirs undergoing waterflood operations to pattern size reduction. Chapter 4 presents the input parameters that went into generating models for a black-oil reservoir simulator (CMG's IMEX). Then, Chapter 5 illustrates the results obtained from reservoir models with various degrees of heterogeneity under different development strategies. Based on these results, conclusions made on the impact of pattern size on waterflood recovery are presented in Chapter 6.

Chapter 2: Engineered Waterdrive

2.1 HISTORY

Waterflooding was discovered over a century ago when water from a shallow aquifer leaked behind the packer of a well to the reservoir. Consequently, an improvement in productivity was realized in nearby production wells (Craft and Hawkins, 1991). However, the use of water injection as an improved recovery technique didn't flourish until the 1950's. During that time period, the oil industry was booming after the discovery of several large fields in west Texas. These solution-gas drive carbonate reservoirs were developed with a spacing of 40 acres per production well; adhering with the guidelines of the Texas Railroad Commission.

After a few years of production, oil rates plummeted because of the drop in reservoir pressure. It was then that operators opted to improve oil productivity through water injection. Initially, peripheral injection patterns were implemented by converting production wells along the field margins into water injection wells. However, reservoirs did not exhibit the desired response from injection. No significant improvement in productivity was realized primarily because of the tight nature (low permeability) of these reservoirs.

Then came the implementation of pattern flooding techniques; interspersed production wells were converted into water injection wells. However, although fruitful, conversion of these producers into injectors resulted in a spacing larger than 40 acres per production well. Infill drilling of producers, combined with the conversion of more producers into injectors, commenced to restore the original 40 acre per producer spacing. This pattern size reduction led to an improvement in productivity as well as an increase in estimated ultimate recovery. (Gulick and McCain, 1998)

2.2 PURPOSE

Waterflooding is an improved oil recovery method used to maintain (or increase) reservoir energy and sweep the oil towards production wells. Water injection can be instigated at production start-up for pressure maintenance or at a later stage in production as a secondary recovery technique. The typical primary recovery expected from solution-gas drive reservoirs is about 15% of the original oil in place (OOIP). Whereas, average recovery from water drive reservoirs is on the order of 40% of the OOIP. In the absence of natural aquifer support, reservoir energy dissipates with production in primary recovery, and fluid injection is required to restore it. The reason behind water being the preferred fluid of choice is its inexpensiveness.

2.3 WATER INJECTION PERFORMANCE

The success of waterflood operations depends on several factors including reservoir properties, fluid properties, as well as development and operation strategies.

2.3.1 Reservoir Properties

The reservoir characteristics impacting waterflood performance include porosity, oil saturation, permeability, structure and heterogeneity. Porosity and oil saturation control the quantity of oil present in a reservoir of a given size. From an economic standpoint, the available reserves should be sufficient to justify the cost of drilling injectors. Also, the reservoir should be permeable enough for the injected water to displace the oil towards the production wells in a timely manner. Otherwise, significant quantities of oil could be left behind at an economic limit. Reservoir structure, particularly dip, can also have an influence on waterflood performance. In dipping reservoirs, designing a water injection scheme that capitalizes on gravity effects can

improve oil recovery. The final and most important reservoir characteristic impacting waterflood performance is heterogeneity.

2.3.1.1 Heterogeneity

Homogeneous reservoirs do not exist in nature. All reservoirs have some degree of complexity/heterogeneity that varies depending on depositional environment and diagenesis. This heterogeneity affects oil recovery by impacting both vertical and areal sweep. Figure 2.1 illustrates the influence of reservoir heterogeneity on oil recovery in different clastic systems. The more heterogeneous the reservoir the smaller the expected oil recovery.

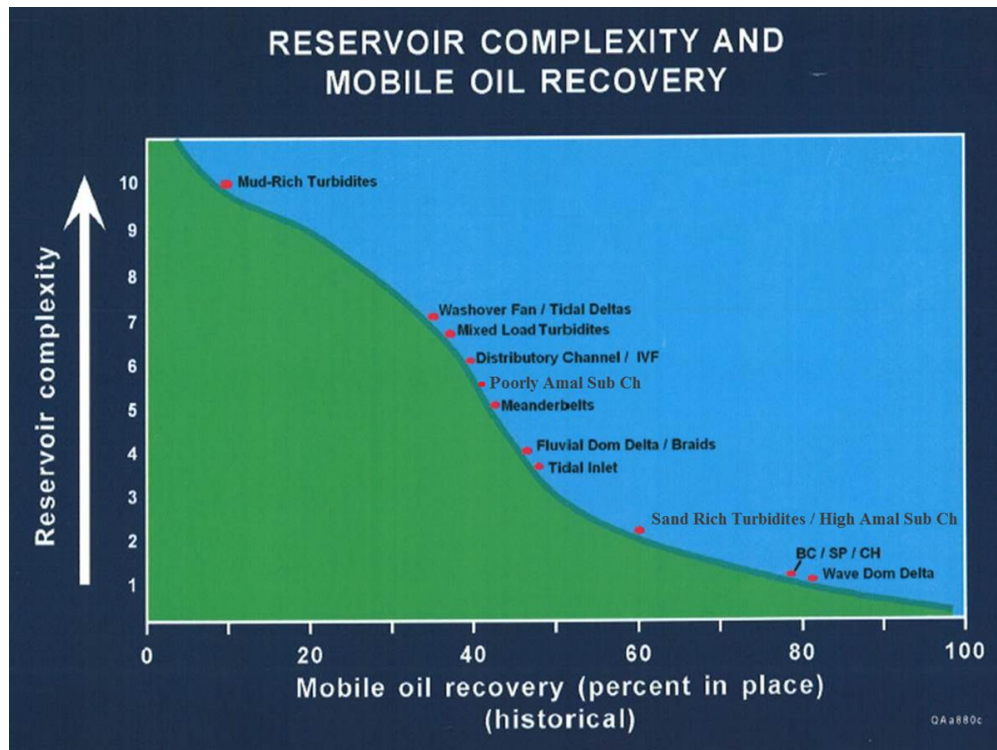


Figure 2.1: Mobile Oil Recovery as a Function of Reservoir Heterogeneity for Different Clastic Reservoirs (Fisher, 2013).

Vertical heterogeneity refers to the variation of petrophysical properties such as porosity, water saturation and permeability with depth. While porosity and water saturation do vary with depth, the variation in permeability is much larger (Dake, 1994). This vertical variation in reservoir properties can be observed in cores and borehole logs collected from drilled wells.

Formation properties such as porosity, water saturation, height and permeability also vary laterally within a reservoir. The existence of reservoir features such as sealing faults and fracture systems can have a strong influence on areal sweep. Vertical heterogeneity can be directly observed through logs and core samples. The characterization of areal heterogeneity is not as direct. Observations of vertical heterogeneity from individual wells are typically extrapolated onto the rest of the field to construct reservoir flow units. This method of flow unit construction is done by correlating similar rock attributes from one well to the other by assuming horizontal flow units and uniform variation of rock properties in-between wells. However, that is rarely true and waterfloods planned based on such assumptions more often than not result in poor areal sweep. Reservoirs can drastically change in-between wells, and better understanding of facies architecture is needed to place producers and injectors in communicating sections of the reservoir.

Figure 2.2 shows one example of how better understanding of reservoir geology can be used in constructing more representative flow units. Based on core data, the depositional setting of the reservoir was interpreted to be that of shallow shelf carbonates (Fisher, 2013). A conceptual depositional model for these types of reservoirs was then used to correlate flow units across the reservoir. In this example, further development based on the new correlation resulted in a substantial improvement in waterflood performance (results from this specific field will be shown in the upcoming development

strategies section). In addition to depositional models, 3-D seismic data can be used to interpret the geometry of flow units. Waterflood performance and well testing can also be used to understand reservoir continuity. However, unlike vertical heterogeneity, the mentioned characterization methods for areal heterogeneity are indirect and will always involve some uncertainty.

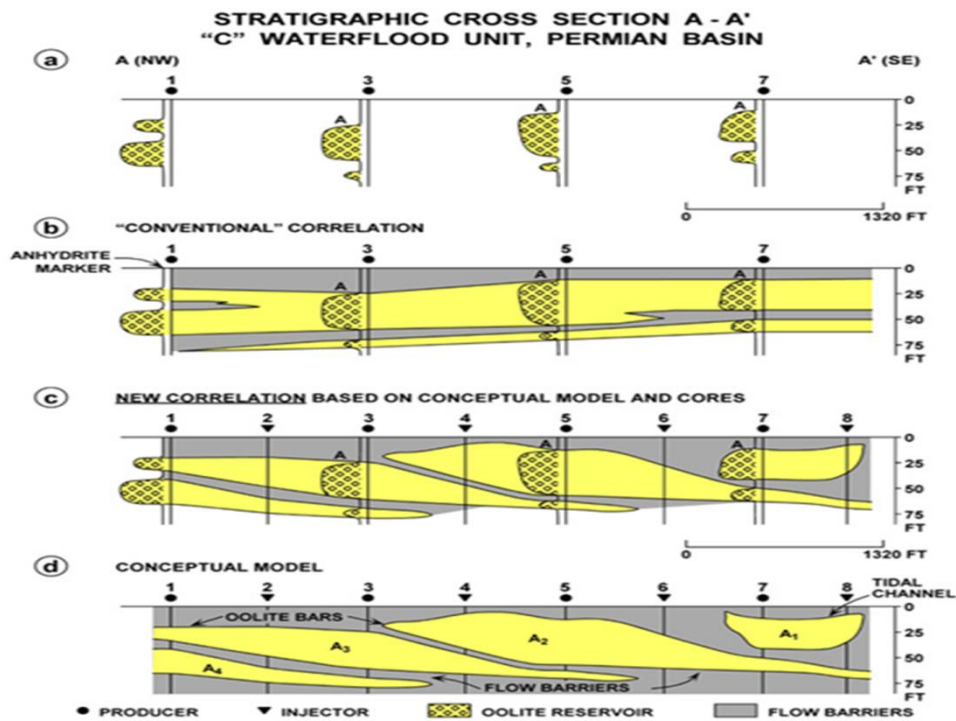


Figure 2.2: Stratigraphic Correlation Based on Better Understanding of Reservoir Geology (Fisher, 2013).

2.3.2 Fluid Properties

In water drive reservoirs (natural and artificial), oil viscosity is the fluid property with most influence on sweep efficiency. Oil viscosity controls mobility ratio (M), which is defined as the mobility of the displacing phase divided by that of the displaced phase.

$$M = \frac{k_{rw}/\mu_w}{k_{ro}/\mu_o} \quad (1)$$

Where M is the endpoint mobility ratio of the oil/water system, k_{rw} is the relative permeability to water, μ_w is the water viscosity, k_{ro} is the relative permeability to oil and μ_o is the oil viscosity. In homogeneous rocks, stable displacement of oil by water occurs at mobility ratios less or equal to 1. At high reservoir oil viscosity, mobility ratio will be larger than 1 causing viscous fingering, which results in early water breakthrough and bypassing oil in the reservoir (Craft and Hawkins, 1991).

Another fluid property that could impact waterflood performance is the bubble point pressure. When reservoir pressure drops below the bubble point, gas is released from solution forming a free-gas phase in the reservoir. The response of waterflooding after this point is postponed until the gas dissolves back into the crude. This delay adversely impacts project economics. Also, oil viscosity is increased because of the loss of solution gas, which reduces oil productivity and results in an unfavorable mobility ratio as explained in the previous paragraph. (Gulick and McCain, 1998)

2.3.3 Development Strategies

Development strategies in waterfloods refer to the placement of production and injection wells. That involves the selection of pattern type, pattern size and well completions.

When it comes to waterflood pattern selection, the first decision to be made is whether to select peripheral flooding or pattern flooding. Peripheral flooding is typically selected for reservoirs with sufficient dip such as anticlinal reservoirs. In peripheral flooding, injectors are completed below the oil water contact as illustrated in Figure 2.3.

Pattern flooding on the other hand, is the preferred development scheme for reservoirs with low dip, large areas, and low permeability. In pattern flooding, injectors are placed in-between producers within the reservoir. Some of the most common pattern flood configurations are shown in Figure 2.4.

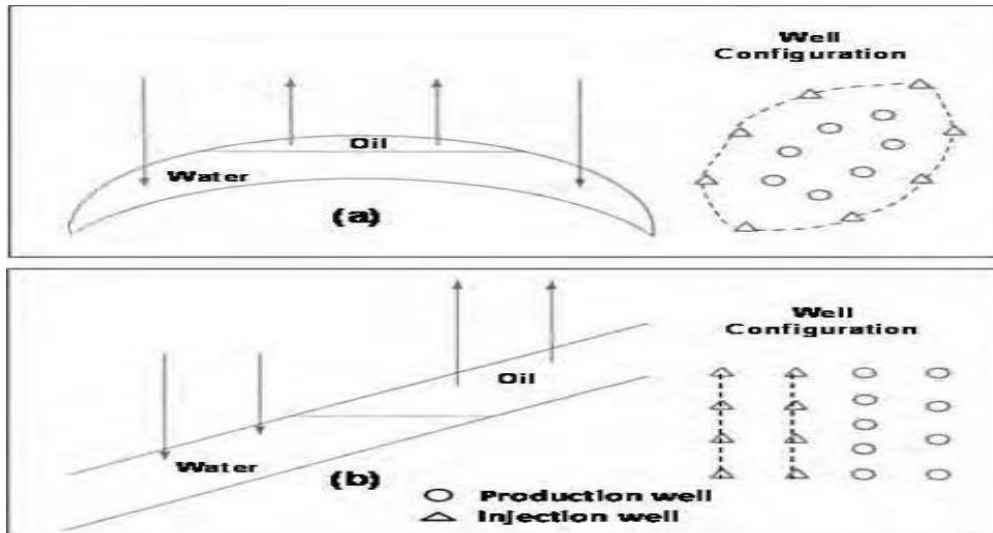


Figure 2.3: Peripheral Water Injection Examples (Craft and Hawkins, 1991).

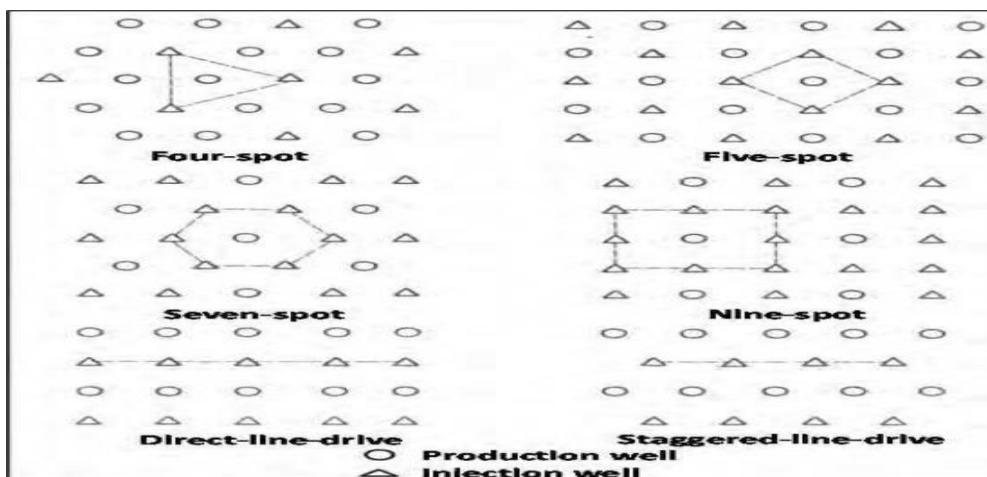


Figure 2.4: Well Locations in Some Common Pattern Floods (Craft and Hawkins, 1991).

Because of their lower investment cost, patterns with a producer to injector ratio of 1 (direct-line drive, staggered-line drive and five-spot) have been used more frequently than others (Craft and Hawkins, 1991). In addition, five-spot and line drive patterns have proven to be more successful than others in heterogeneous reservoirs (Gulick and McCain, 1998). The orientation of such patterns can also be crucial to waterflood performance whenever directional permeability trends or natural fracture systems exist. Also, induced fracture orientation should be taken into account when selecting waterflood pattern orientation. The alignment of producers and injectors should not follow the induced fracture orientation. Otherwise, injecting above the formation's fracturing pressure will result in premature water encroachment at the producers (Gadde and Sharma, 2001).

Prior to reviewing the literature related to the effect of pattern size on waterflood recovery, a distinction should be made between pattern size and well spacing (or density). Pattern size can correspond to a different well spacing, depending on the type of flooding pattern. For example, in a five-spot pattern, well spacing is half the pattern size, whereas well spacing in a 9-spot pattern is four times the pattern size (Lyons, 1996). Pattern size reduction accelerates oil production thereby reducing recovery time. Whether reducing pattern size increases ultimate recovery or not will be more thoroughly examined in the upcoming chapters of this thesis.

In the past, many production wells were only completed in the highest permeability zones. However, these high permeability zones do not necessarily correlate between different wells. The conversion of some of these producers into injectors and the commencement of waterflooding will result in bypassed oil in low permeability zones

(Gulick and McCain, 1998). It is therefore vital to perforate across the entire reservoir in both production and injection wells to optimize waterflood performance.

Based on better understanding of the reservoir shown in Figure 2.2, the field was developed with some of the above-mentioned strategies. The reservoir's response to the change in development strategy is illustrated in Figure 2.5, where major events are designated with letters A-D. The field was initially developed with a spacing of 40 acres per production well. At point **A**, oil production began declining because of the lack of pressure support. Peripheral waterflooding was then instigated at point **B**. However, peripheral injection did not yield the desired improvement in productivity. Later, at point **C**, a 20 acre five-spot pilot was initiated in a section of the field. Encouraging results from the pilot paved the way for a field-wide implementation. At point **D**, pattern size was reduced from 40 acres per production well to 20 acre per well in a five-spot pattern, and all the pay zones were perforated. The result was a tripling in the ultimate oil recovered from 90 million barrels to 265 million barrels (Fisher, 2013).

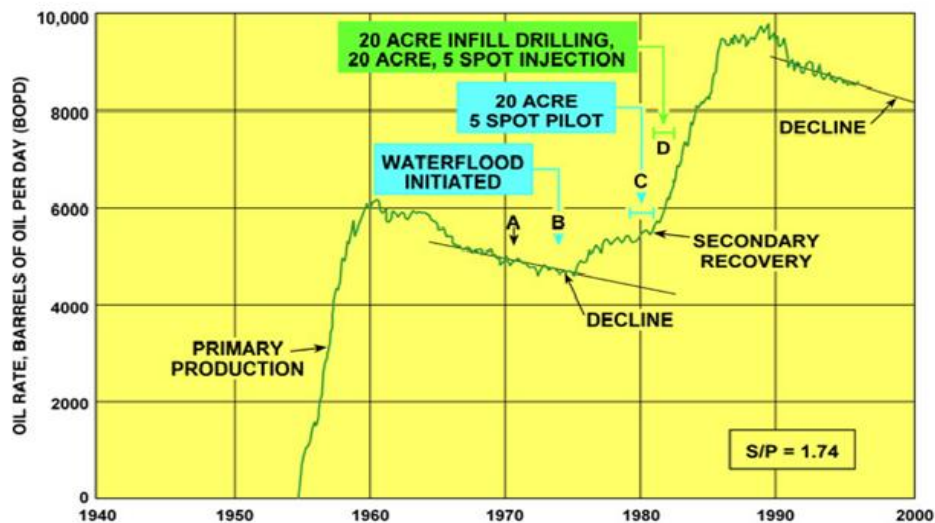


Figure 2.5: Field Performance of a Shallow Shelf Carbonate Reservoir (Fisher, 2013).

2.3.3 Operation Strategies

Waterflood performance can also be improved through the execution of certain operation strategies which include maintaining pressure above the bubble point pressure, injecting below the fracturing pressure, injecting clean water, conducting well tests on injection wells and implementing a comprehensive surveillance program (Gulick and McCain, 1998).

Chapter 3: Literature Review

3.1 FIELD PERFORMANCE DATA

Numerous studies have examined the impact of pattern size reduction on field performance through decline curve analysis. This chapter reviews the published literature, in chronological order, specifically pertaining to water drive (natural or engineered) reservoirs.

3.1.1 Little Buffalo Basin Field

The Little Buffalo Basin Field, located in the north-west region of Wyoming, produces hydrocarbons from 5 reservoirs on its anticlinal structure. The Tensleep reservoir is a 4,600 ft deep natural water drive reservoir that produces a 20° API crude with a viscosity of 42 centipoise (cp). This 275-300 ft thick reservoir is composed of an upward coarsening sand body with interbedded limestone and dolomite; interpreted to be deposited in a deltaic setting. The dolomite layers are impermeable and laterally discontinuous. However, the presence of vertical fractures allows communication between the sand bodies. Other reservoir heterogeneities include cross-bedding which causes permeability anisotropy. On average, permeability parallel to the cross-bedding was found to be 4 times that of the permeability perpendicular to it. In addition, cementation causes reduction in both porosity and permeability. The reservoir's average porosity is 14% and its average permeability is 61.3 milli-Darcies (md). However, permeability varies both vertically and horizontally from 0-1,150 md (Emmett et al., 1971).

The Tensleep reservoir was initially developed with a spacing of 40 acres per production well. However, poor performance was observed in wells placed in the heavily fractured northern and western areas of the field. These wells were producing directly

from open fracture systems connected to the aquifer. Intuitively, this resulted in early water breakthrough and the bypassing of matrix oil. In addition, other areas of the field were also suspected of having poor sweep mainly because of directional permeability trends and an unfavorable mobility ratio. As a result of these findings, the operators elected to increase well density. From 1966-1970, the drilling of an additional twenty six wells reduced the pattern size from 40 to 20 acres. Figure 3.1 demonstrates how this further development was successful in arresting the production decline. In addition to accelerating production, pattern size reduction was reported to have increased ultimate recovery by **5% of the original oil in place** (Emmett et al., 1971).

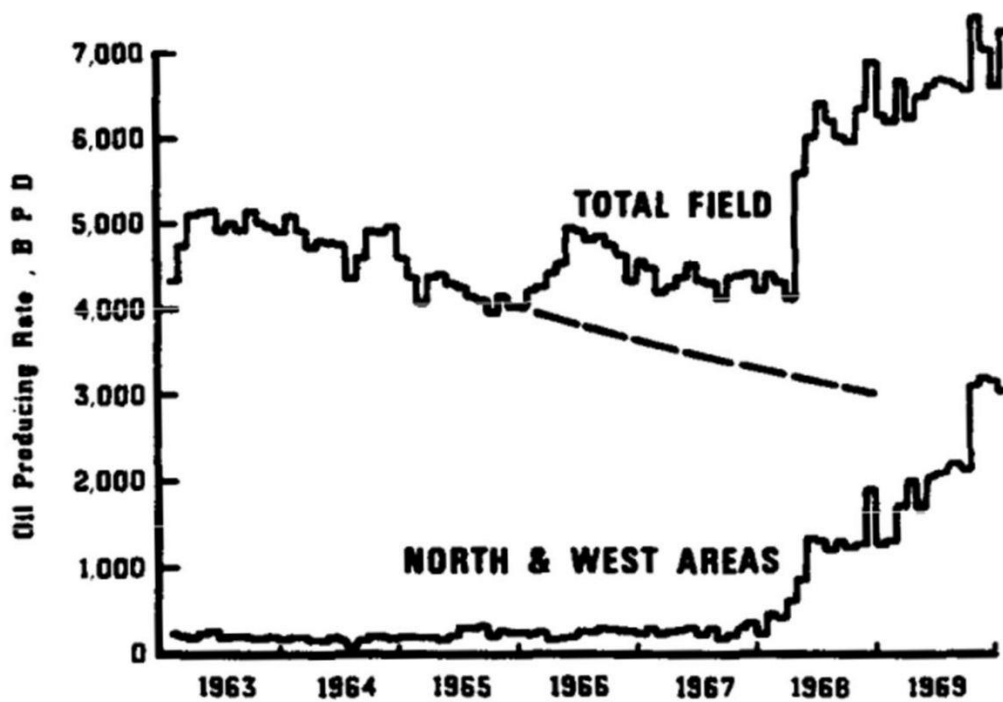


Figure 3.1: The Effect of Pattern Size Reduction on the Performance of Little Buffalo Basin's Tensleep Reservoir (Emmett et al., 1971).

3.1.2 Yates-Queen Sand

Production from this unnamed west Texas field is primarily from of the Yates and Queen sands. The productive interval, located between a depth of 2,600-3,200 ft, consists of sands and shaley sands interbedded with dolomite. Produced oil has a stock tank gravity of 32° API and a low viscosity of 1.39 cp (Driscoll, 1974).

Prior to pattern size reduction, the majority of the 320 acre lease was developed with a 40 acre five-spot waterflood pattern. However, there were a few areas with 10 acre five-spots and others with 20 acre five-spots. The total well count at the time was 860 wells including 350 injectors. The pattern size was then reduced by drilling an additional 247 producers. This pattern size reduction increased reservoir continuity which resulted in improving waterflood recovery as illustrated in Figure 3.2 below. The estimated ultimate oil recovery increased by **14.6 million barrels** corresponding to an **additional 5.4% of OOIP** (Driscoll, 1974).

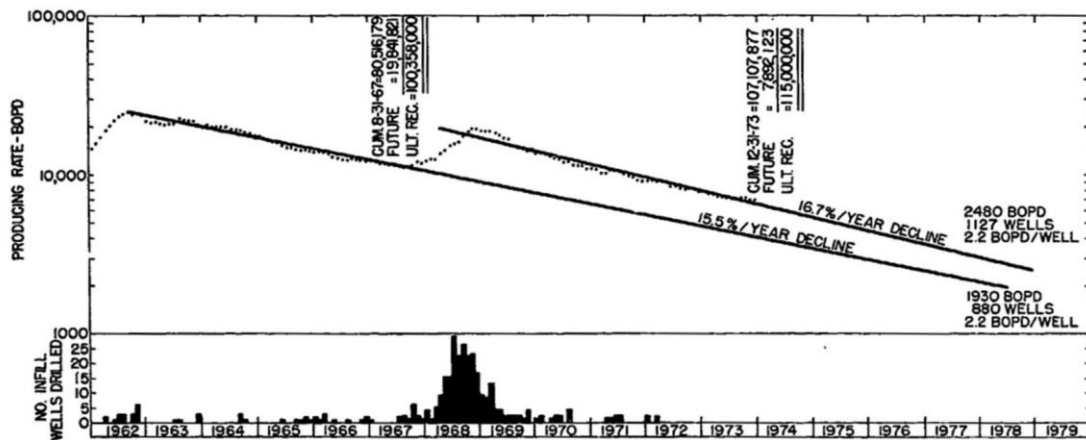


Figure 3.2: Waterflood Response to Pattern Size Reduction
Yates-Queen Sands (Driscoll, 1974).

3.1.3 Grayburg Dolomite

Located in west Texas, this 800 acre area produces oil from a 230 ft Grayburg dolomite reservoir. Permeability in the reservoir ranges between 1 to 5 md and the produced crude has a viscosity of 1.5 cp. Waterflooding commenced with an 80 acre five-spot development for most of the field. However, this waterflood resulted in a rapid increase in watercut and a poor oil response as shown in Figure 3.3. Investigation later revealed that this poor performance was attributed to the presence of natural and induced fractures that connected injection wells to production wells. Based on production decline, the waterflood recovery was estimated to be a mere **18.6% of OOIP**. In response, infill drilling of 17 new wells reduced the five-spot pattern size from 80 acres to 40 acres. The five-spot pattern orientation was also altered to target the bypassed matrix oil. Pattern size reduction and realignment resulted in a gain of **2.4 million barrels** of oil, which increased recovery to **28.5% of OOIP** (Driscoll, 1974).

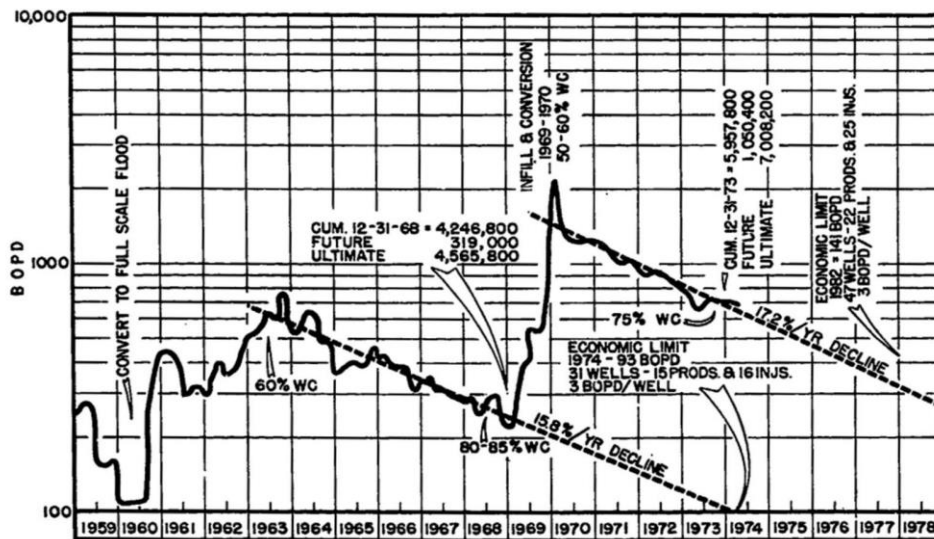


Figure 3.3: The Impact of Decreasing Pattern Size on Oil Production from a Grayburg Dolomite Reservoir (Driscoll, 1974).

3.1.4 Slaughter Field

The Slaughter Field is a 99,000 acre producing area that spreads across Hockley, Cochran and Terry counties of west Texas. Oil production is from a 51 ft thick heterogeneous limestone/dolomite reservoir undergoing water injection. The reservoir has an average porosity of 10.8% and an original oil in place of 2.8 billion barrels. Different units within this large field are developed with different flooding pattern sizes. Figure 3.4 demonstrates the existence of a relationship between pattern size and ultimate waterflood recovery in The Slaughter Field. The overall trend indicates that oil recovery increases as pattern size decreases. At a single pattern size, different units can have substantially diverse recovery efficiencies because of their different reservoir characteristics. However, fitting any trendline between the data indicates that recovery can be doubled by increasing well density from 40 to 20 acres per well (van Everdingen, 1980).

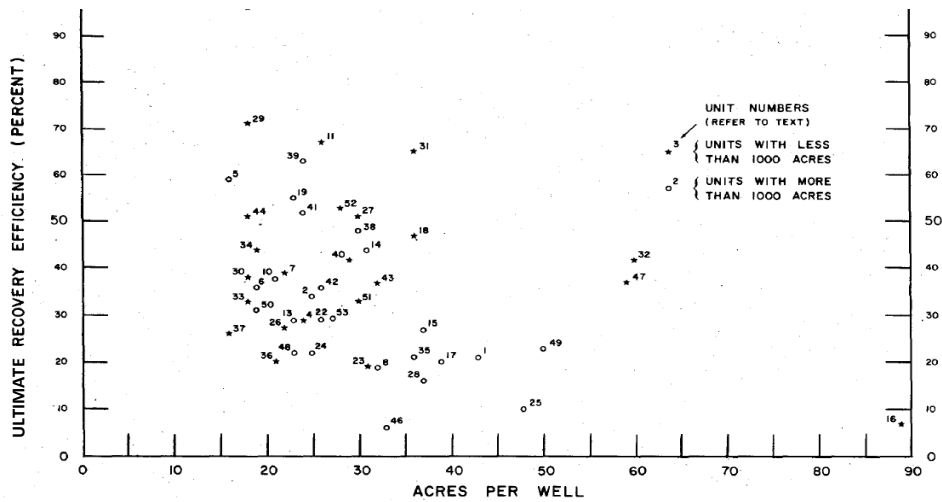


Figure 3.4: Waterflood Recovery as a Function of Well Spacing in Slaughter Field (van Everdingen, 1980).

3.1.5 Permian Basin Units

A study published by Kern in 1981 examined the effect of well spacing on waterflood recovery in 48 Permian Basin units. Oil recovery was plotted versus well spacing in a similar manner to Figure 3.4 above. However, no clear relationship was established between spacing and waterflood recovery. The 48 units were then divided into permeability groups and the effect of well spacing on each group was analyzed separately. Waterflood recovery was found to correlate with pattern size for units with permeabilities lower than 0.8 md. However, no relationship was observed between recovery efficiency and well spacing in high permeability (> 0.8 md) units. Figures 3.5 and 3.6 clearly indicate that low permeability units with a denser well spacing have higher oil recovery efficiency (Kern, 1981).

Permeability values referenced in this study were not obtained through core measurements but through rough approximations based on production flow rates. This fact could indicate that permeability in this case refers to reservoir heterogeneity, the lower the permeability the more heterogeneous the reservoir (Kern, 1981). Other studies pertaining to Permian Basin fields (Gulick and McCain, 1998) and (Barber et al., 1983) stress the concept of reservoir discontinuity. It could be that the higher ultimate recovery efficiency resulting from pattern size reduction in low permeability units (< 0.8 md) is because of increasing reservoir continuity.

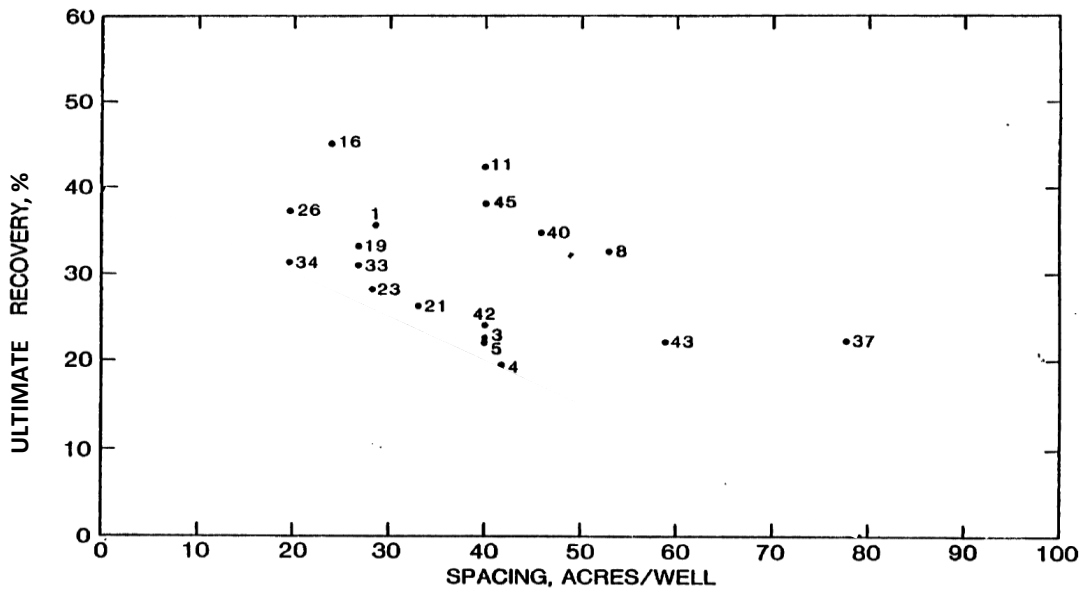


Figure 3.5: Waterflood Recovery as a Function of Well Spacing for Permian Basin Units with Reservoir Permeability Ranging from 0.4 md to 0.8 md (Kern, 1981).

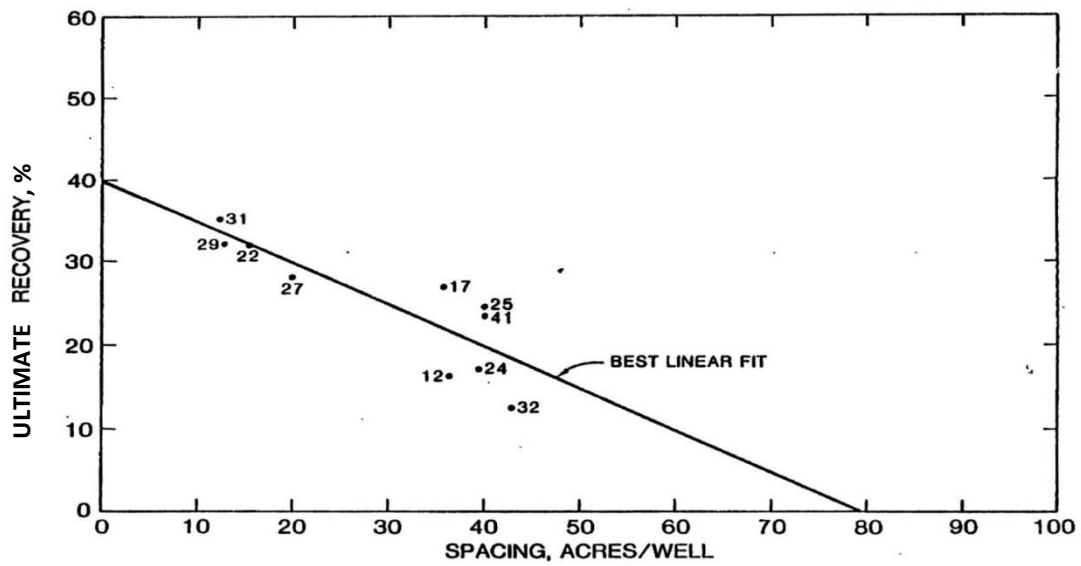


Figure 3.6: Waterflood Recovery as a Function of Well Spacing for Permian Basin Units with Reservoir Permeability Lower than 0.4 md (Kern, 1981).

3.1.6 Means San Andres Unit

Located in Andrews County, Texas, the Means Sand Andres unit produces from a 4,400 ft deep dolomite reservoir with 200-300 ft of pay. The reservoir consists mainly of dolomite with some shale and anhydrite. Furthermore, the average porosity is 8%, the average permeability is 20 md and the produced oil viscosity is 6 cp. Pattern waterflooding began when the field was developed with 40 acre three-to-one line drive patterns. Afterwards, infill drilling of 141 production wells reduced well spacing to 20 acres per well. This increase in well density resulted in a gain of **15.4 million barrels**. In a smaller area of the field, the drilling of 16 additional producers decreased well spacing to 10 acres per well and resulted in an additional oil recovery of **1.2 million barrels**. In this example, the improvement in oil recovery resulting from increasing well density is attributed to contacting pay zones that have been previously isolated (Barber et al., 1983).

3.1.7 Fullerton Field

Also located in Andrews County, Texas, oil production in the Fullerton field is from the Permian Clearfork and Wichita formations. The reservoir is characterized as being a dolomite with interbedded limestone, anhydrite and shale. The pay zone is 7,000 ft deep with an average porosity of 10%, an average permeability of 3 md and a low oil viscosity of 0.75 cp. Prior to pattern size reduction, the field was developed with a 40 acre three-to-one line drive. Additional development reduced pattern size by infill drilling of production wells and by converting of some of the original producers to injectors. The new producers exhibited higher production rates and lower watercuts than the original wells indicating that new pay zones were being contacted. The additional oil recovered from this new development strategy was estimated to be **24.6 million barrels** (Barber et al., 1983).

3.1.8 Robertson Field

The Clearfork Unit of the Robertson Field is located in Gaines County, Texas. Oil production is from the Upper Clearfork, Lower Clearfork and Glorieta formations. The reservoir is 6,500 ft deep and is composed primarily of dolomite with interbedded anhydrite and shale. Log data indicates that the 200-300 ft pay zone is broken up into numerous separate vertically stacked layers. The reservoir has an average porosity of 6.3%, an average permeability of 0.65 md, and an oil viscosity of 1.2 cp. The area was initially drilled on 40-acre spacing, and water injection was instigated to improve recovery. Infill drilling then increased well density to 20 acres per well in most areas of the field. In other areas, spacing was further reduced to 10 acres per well. As a result, an additional **10.7 million barrels** of oil are expected to be realized (Barber et al., 1983).

3.1.9 IAB Field

The IAB Field, located in Coke County, Texas, produces oil from the 5,800 ft deep Menielle Penn reservoir. This limestone reservoir has an average porosity of 7% and an average permeability of 27 md. Moreover, oil viscosity at reservoir conditions is 0.2 cp. Upon discovery, the field was drilled on 80 acre spacing. Waterflooding later began with a three-to-one line drive pattern. Subsequently, additional development reduced the spacing to 40 acres per well which resulted in increasing reserves by **1.7 million barrels (4% of OOIP)** (Barber et al., 1983).

3.1.10 Howard-Glasscock Field

The Douthit Unit of the Howard-Glasscock Field is located in Howard and Sterling Counties, Texas, and produces oil from the 1,400 ft deep Seven Rivers reservoir. This sandstone reservoir has an average porosity of 18%, an average permeability of 44 md, and an oil viscosity of 9.4 cp. Initially, the area was developed on 40 acre spacing,

and waterflooding began with a peripheral injection pattern. Then, infill drilling of production wells reduced the pattern size to 10 acres. As a result, estimated oil recovery increased by **1 million barrels** (Barber et al., 1983).

3.1.11 Hewitt Field

The Hewitt Field is located in Carter County, Oklahoma, and produces oil from the Hoxbar and Deese sands. The 1,500 ft thick reservoir is comprised of 22 sand bodies that are vertically separated by shales. Pay zones have an average porosity of 21%, an average permeability of 184 md and a crude viscosity of 8.4 cp. Waterflooding began by developing the field with 20 acre five-spot patterns. Then, the drilling of an additional 15 producers reduced the well spacing to 5 acres per well. This pattern size reduction resulted in a gain of **400,000 barrels of oil** (Barber et al., 1983).

3.1.12 Loudon Field

Located in Fayette and Effingham Counties, Illinois, the Loudon Field produces oil from a 1,500 ft deep sandstone reservoir. Sand bodies have an average porosity of 19% and an average permeability of 100 md. Moreover, oil viscosity is 5 cp at reservoir conditions. Water injection began by developing the field with 70 acre nine-spot patterns in the north and 20 acre five-spot patterns in the south. Further development then converted the 70 acre nine-spot patterns into 10 acre five-spot patterns. Subsequently, 50 infill production wells were drilled and resulted in increasing oil recovery by **970,000 barrels** (Barber et al., 1983).

3.1.13 El Morgan Field

Egypt's El Morgan Field is a giant offshore oil field located in the Gulf of Suez. Oil is predominantly produced from the 10,000 acre Kareem sandstone reservoir. The structure of the reservoir consists of an anticline bounded by a sealing normal fault. The

Kareem reservoir was initially believed to be a 950 ft thick homogeneous sand body with a porosity of 22.8% and a permeability of 640 md (Mahmoud, 1987).

Upon discovery, the field was populated with production wells with the assumption that influx from an underlying active natural aquifer would sustain the reservoir's energy. However, because of high production rates, reservoir pressure began to decline. In response, peripheral water injectors were drilled and waterflooding was initiated. This implementation of secondary recovery operations was successful in arresting the pressure decline. Nonetheless, it was suspected that a substantial amount of oil was being bypassed. This suspicion was later confirmed through cores, logs and pressure surveys (Mahmoud, 1987).

The reservoir proved to be much more heterogeneous than originally anticipated. Core analysis indicated the presence of 5 different rock types, which vary in reservoir quality. Furthermore, flowmeter surveys in water injectors showed ununiform injection profiles because of rock characteristics. Additionally, reservoir pressure was found to vary significantly in different wells. As a result of these findings, well density was increased to improve vertical and areal sweep efficiencies. The drilling of additional production and injection wells is expected to increase oil recovery by **200 million barrels**, which corresponds to an **8.5% improvement in recovery** (Mahmoud, 1987).

3.1.14 McElroy Field: Section 205

The McElroy Field is located in Crane and Upton Counties, Texas. Section 205 is located in the southwestern region of the field. In this area, oil is produced from the Grayburg and San Andres dolomites. The Grayburg is 3,000 ft deep and is the main formation undergoing waterflood operations. Oil is confined in the reservoir through structural and stratigraphic trapping mechanisms. The McElroy structure is an

asymmetrical anticline trending to the north. Moreover, an impermeable flow barrier is located on the west flank of the field. Porosity in Section 205 of the Grayburg dolomite ranges from 8% in the west to 16% in the east. Conversely, permeability varies from 1 md in the west to 50 md in the east. Furthermore, the reservoir is characterized as being both vertically and laterally discontinuous (Lemen, 1990).

Prior to pattern reconfiguration, the field was developed with 40 acre inverted nine-spot patterns in the southwest and 80 acre octagon (sunflower) patterns in the southeast and northeast. Under this development strategy, production wells exhibited a drop in productivity and low bottom-hole pressures. Both of these observations were attributed to reservoir discontinuity. Additionally, early water breakthrough in certain production wells indicated that the reservoir had a favorable flooding direction. Studies later confirmed that this directional permeability trend was caused by induced fractures (Lemen, 1990).

In an attempt to improve waterflood performance, a decision was made to convert the field's development to 20 acre five-spot patterns. In addition to increasing reservoir continuity, producers and injectors were strategically placed to minimize the effect of the N60°W directional permeability trend. The impact of this pattern reconfiguration project is demonstrated in Figure 3.7 below. As a result of this new development strategy, the production decline was arrested thanks to adequate pressure support from the water injectors. The additional gain in oil recovery from this project is estimated to be **951,000 stock tank barrels** (Lemen, 1990).

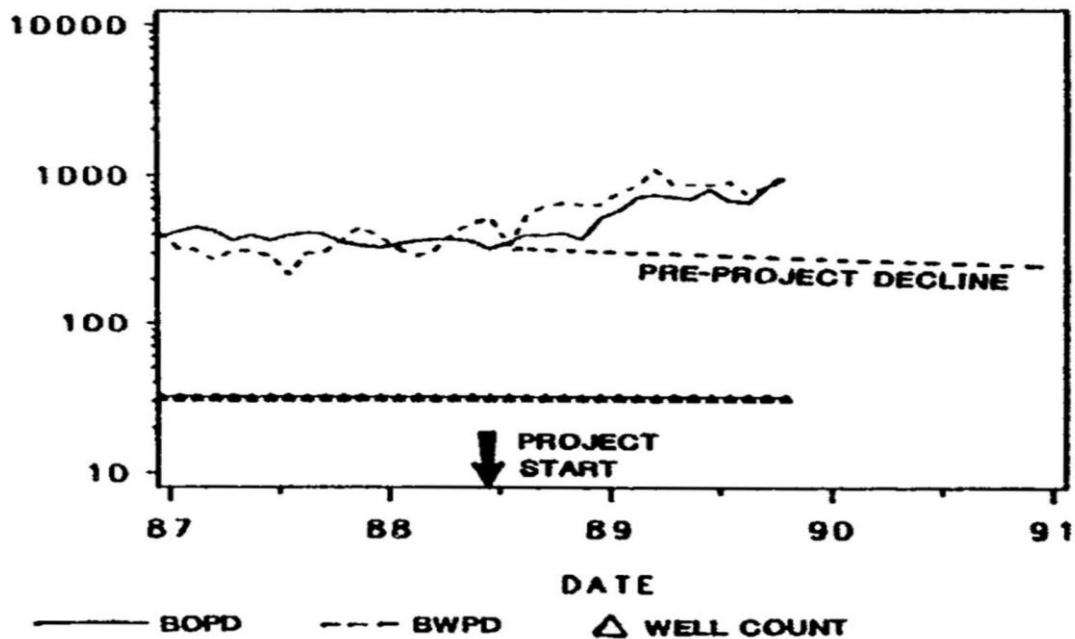


Figure 3.7: The Impact of Pattern Realignment on Oil Production and Water Injection on Section 205 of the McElroy Field (Lemen, 1990).

3.1.15 Prudhoe Bay Field

Located in Alaska's North Slope, the Prudhoe Bay Field has a surface area of 250 square miles with original oil in place estimates exceeding 22 billion barrels. Oil is produced from the reservoir through several artificial drive mechanisms including waterflooding and water-alternating-gas flooding. Areas undergoing fluid injection recovery techniques are assembled into 4 main groups: the Northwest Fault Block (NWFB), the Western Peripheral Wedge Zone (WPWZ), the Eastern Peripheral Wedge Zone (EPWZ) and Flow Station Two (FS-2).

The effect of well spacing on ultimate oil recovery in each of these groups is illustrated in Figure 3.8. As can be observed in this bar chart, EPWZ and NWFB have the densest well spacing. Furthermore, the highest infill potential exists in the WPWZ. In this

group, reducing well spacing that is larger than 110 acres to less than 90 acres can improve ultimate recovery by 22% OOIP. Whereas, decreasing spacing larger than 85 acres to lower than 76 acres in the EPWZ only enhances ultimate recovery by 6% OOIP. Nonetheless, within each group, areas developed with a denser well spacing demonstrated higher recovery efficiencies than areas with wider spacing (Kwan, 1992).

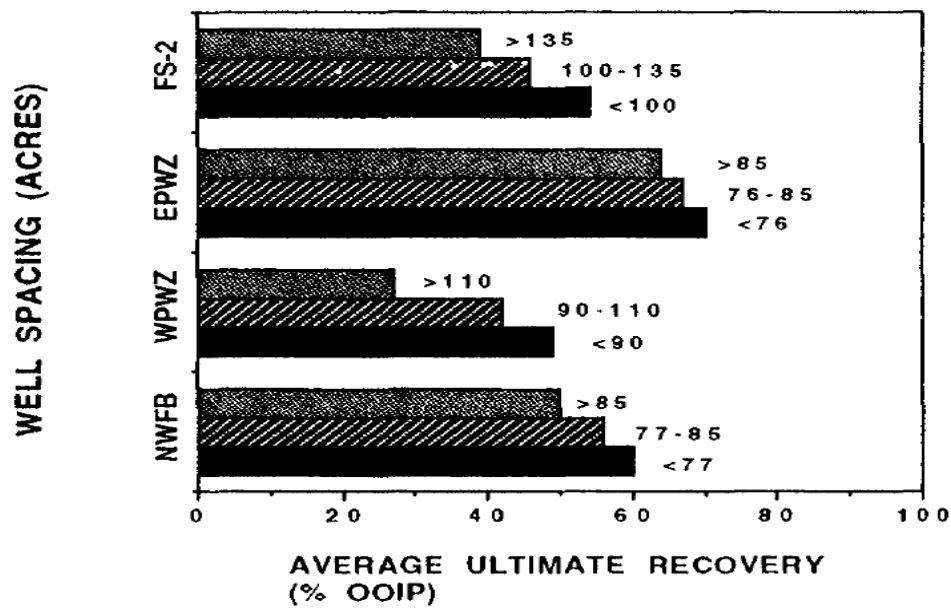


Figure 3.8: The Effect of Well Spacing on Oil Recovery in the Prudhoe Bay Field (Kwan, 1992).

A study conducted on the WPWZ waterflood identified that the presence of several large faults was detrimentally impacting areal sweep efficiency in areas with sparse well density. Pattern size reduction, through drilling additional wells and converting producers to injectors, was selected to enhance waterflood recovery. In the “A” pad area, this strategy is projected to increase oil recovery by **15 million barrels**. Similarly, developing the “Y” pad area with smaller patterns is expected to improve recovery by **16 million barrels of oil** (Suttles and Kwan, 1993).

3.2 RATIONALE

The main underlying theme in the aforementioned studies is reservoir heterogeneity. In fact, most of the studies deemed reservoir discontinuity to be the principal factor causing the improvement in oil recovery realized from pattern size reduction. However, areal pay zone discontinuity is not the only factor that can cause an inverse relationship between pattern size and waterflood recovery. Other factors that influence infill potential include preferential flooding directions, “wedge-edge” oil recovery, irregular pattern geometry, confinement of injected fluids to pay zones, vertical reservoir discontinuity, and project economics (Driscoll, 1974).

3.2.1 Areal Reservoir Discontinuity

The concept of areal reservoir discontinuity, illustrated in Figure 2.2 of the previous chapter, is the most common explanation for the dependence of waterflood recovery on pattern size. In such compartmentalized reservoirs, development with widely spaced patterns increases the probability of certain pay zones being unexploited. Significant quantities of oil can also be left behind by exclusively penetrating certain reservoir compartments by either a production well or an injection well. In the former case, the lack of injection will cause oil production in that particular compartment to exhibit a similar behavior to that of primary recovery operations. Whereas, pay zones only contacted by injectors will be completely unswept.

Reduction of pattern size increases the likelihood of tapping into uncontacted pay zones with both production and injection wells. This concept is illustrated in Figure 3.9, where reservoir continuity is plotted as a function of horizontal distance in the Wasson Sand Andres Field. Reservoir continuity was quantified using a statistical approach described by Stiles (1976). The curve shown in Figure 3.9 was generated using data from 100 wells dispersed throughout the Wasson Denver Unit (Maguson and Knowles, 1977).

In this particular field, reducing the development pattern size from 80 acre five-spots to 40 acre five-spots increased reservoir continuity by 4%, which resulted in increasing oil recovery by **18 million barrels** (Driscoll, 1974).

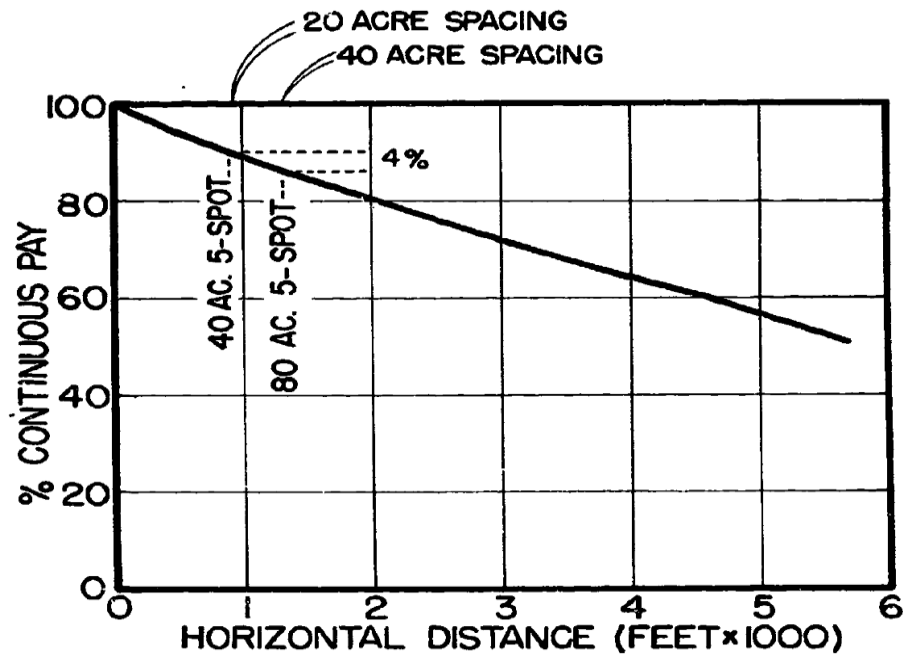


Figure 3.9: Reservoir Continuity as a Function of Horizontal Distance in the Wasson Sand Andres Field (Driscoll, 1974).

3.2.2 Preferential Flooding Directions

Waterflood recovery can strongly be influenced by favorable flooding orientations. While stratigraphy-related permeability anisotropy can give rise to such preferential flooding directions, the presence of natural or induced fractures has a more significant effect on waterflood performance. Figure 3.10 demonstrates how pattern alignment, with respect to fracture orientation, can impact oil recovery. This schematic represents a reservoir with east-west trending fractures that is developed with five-spot patterns. As shown in Figure 3.10, early water breakthrough in the east-west direction

resulted in bypassing oil in the north-south direction. Pattern size reduction in such reservoirs can increase waterflood recovery by improving areal sweep (Driscoll, 1974).

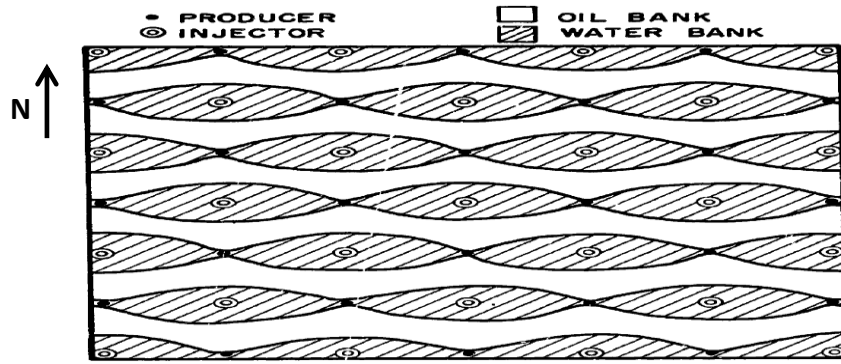


Figure 3.10: Five-Spot Waterflood with East-West Fracture Orientation (Driscoll, 1974).

3.2.3 “Wedge-Edge” Oil Recovery

In fields producing oil from numerous dipping pay zones, development pattern size can impact “wedge-edge” oil recovery. In such reservoirs, underdevelopment in the periphery of the field can cause oil to be trapped close to the oil-water contact. This concept is illustrated in Figure 3.11, where the shaded areas represent unswept oil. In this cross section, the drilling of 2 new injectors is proposed to target the bypassed edge oil and enhance waterflood recovery (Driscoll, 1974).

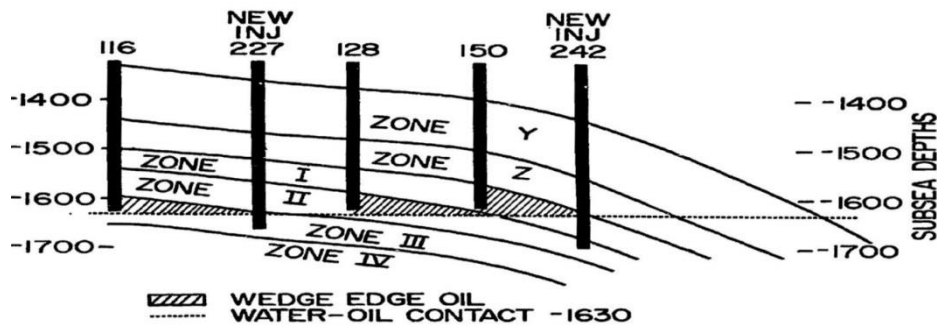


Figure 3.11: Unswept Oil at the Edge of the Field (Driscoll, 1974).

3.2.4 Irregular Pattern Geometry

Even in relatively homogeneous reservoirs, reducing well spacing can improve areal sweep in fields developed with irregular patterns. Thomas and Driscoll (1973) reported that a 3.6% improvement in waterflood recovery is achievable through infill drilling “chickenwire” shaped patterns in Slaughter Field, Texas. The effect of irregular pattern geometry on areal sweep is illustrated in Figure 3.12, where the shaded areas represent unswept oil. The drilling of 6 additional production wells within such patterns reduces the amount of bypassed oil; therefore, enhancing waterflood performance (Driscoll, 1974).

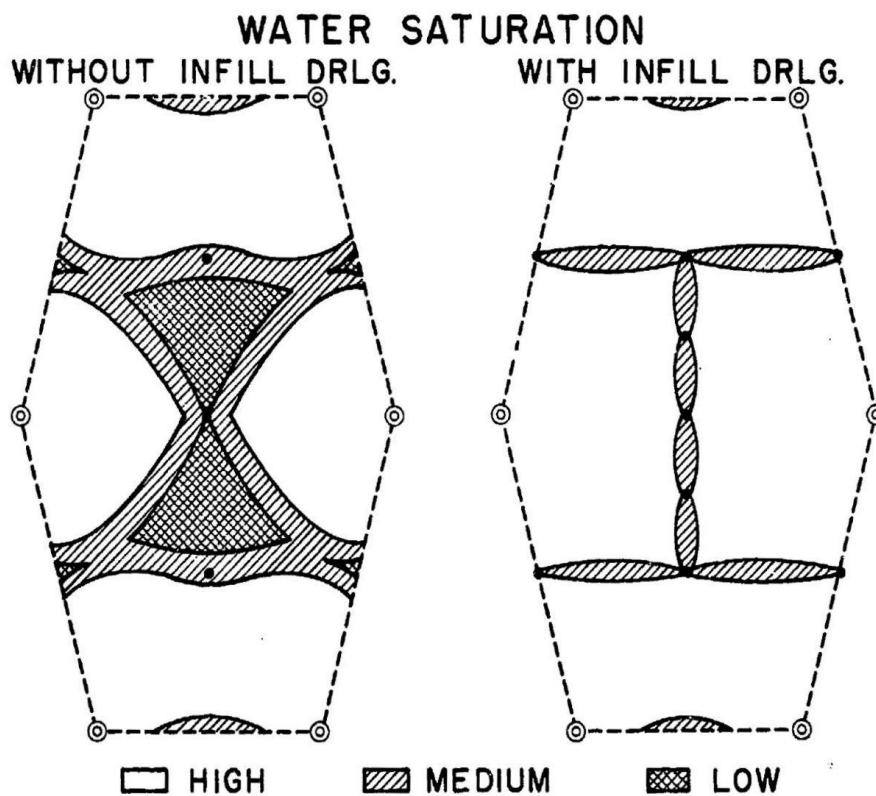


Figure 3.12: The Improvement in Areal Sweep Achieved through Infill Drilling “Chickenwire” Patterns (Driscoll, 1974).

3.2.5 Vertical Communication with Water-Bearing Zones

The confinement of injected water to the pay zone is essential for waterflood success. In several west Texas fields, the loss of injection water to underlying formations was adversely impacting waterflood recovery. Initially, these fields underwent primary recovery operations. Moreover, production wells were hydraulically fractured to maximize production rates. As a result of poor hydraulic fracture design, communication was established with underlying water-bearing zones. When waterflooding commenced, many of these fractured producers were converted into water injectors. As a result, water injected into these wells was not confined to the pay zone (Figure 3.13). In such situations, pattern size reduction can improve waterflood recovery by eliminating communication with underlying (or overlying) aquifers (Driscoll, 1974).

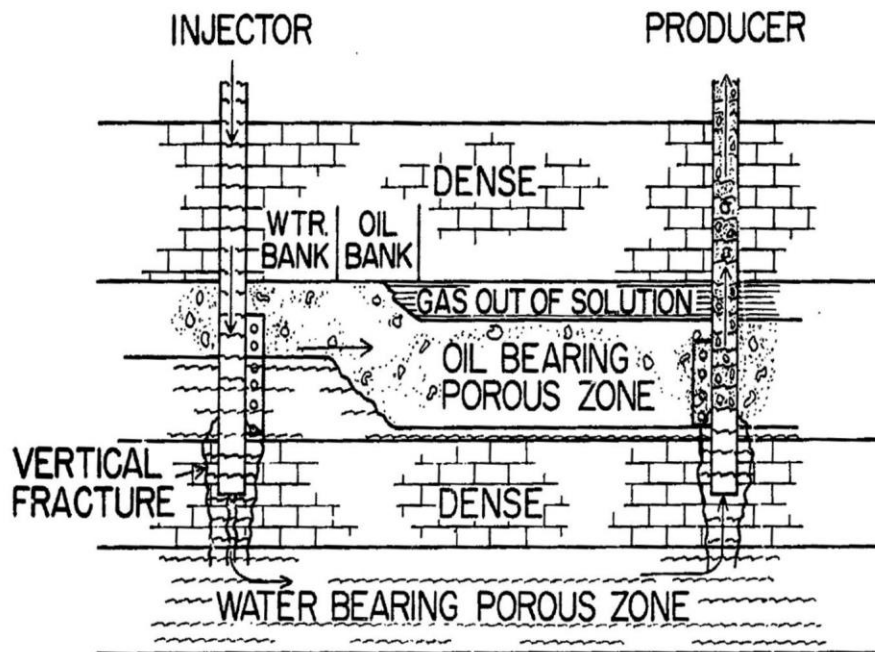


Figure 3.13: Vertical Communication with Water-Bearing Zones (Driscoll, 1974).

3.2.6 Layered Reservoirs

In many fields, oil is produced from numerous vertically discontinuous layers. With both producers and injectors perforated across all the pay zones, vertical sweep becomes dependent on permeability variations between the different layers. Injected water will sweep higher permeability layers at a faster rate than it does lower permeability pay zones. This uneven waterfront advancement causes production wells to water-out; hence, leaving oil behind in low permeability layers (see Figure 3.14). In such situations, the reduction of pattern size can increase waterflood recovery by improving vertical conformance (Driscoll, 1974).

Alternatively, selective injection techniques can be implemented to control injection profiles in layered reservoirs. More uniform injection profiles can also be attained through hydraulically fracturing low permeability pay zones. However, oil has already been bypassed in fields where such strategies have not been employed. In the Wasson Denver Unit, where oil is produced from vertically discontinuous pay zones, a **14 million barrel (1.5% OOIP)** improvement in waterflood recovery is achievable through increasing well density (Shell Oil Co., 1972).

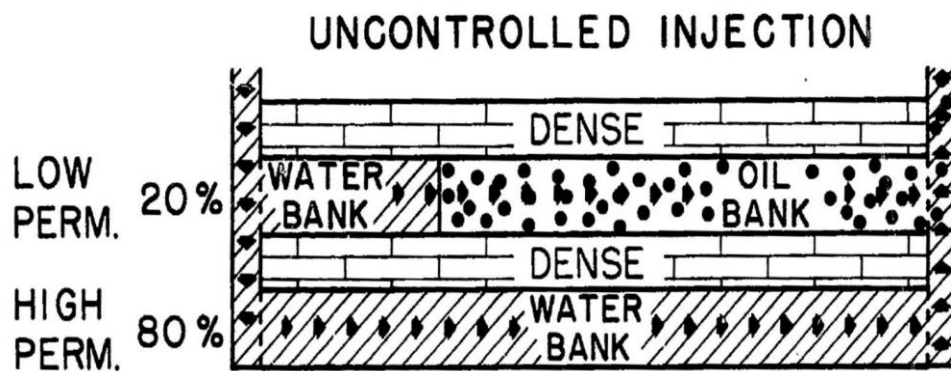


Figure 3.14: Vertically Discontinuous Pay Zones with (Driscoll, 1974).

3.2.7 Project Economics

The acceleration of oil production associated with pattern size reduction can result in recovering incremental oil at field abandonment rate. This effect is more prominent in reservoirs with low formation capacity. Figure 3.15 shows waterflood recovery as a function of formation capacity for 2 different flooding pattern sizes in the Levelland Unit, Hockley County, Texas. For the 85 acre five-spots, the economic limit rate per well was selected to be 10 barrels of oil per day (BOPD/well). Whereas, because of the larger number of producers associated with tighter patterns, an economic limit of 9 BOPD/well was selected for the 42.5 acre five-spots. Given these conditions, Figure 3.15 illustrates the projected gain expected from pattern size reduction. At a formation flow capacity (kh) of 320 md-ft, a **1% OOIP** improvement in waterflood recovery is expected from reducing development pattern size from 85 acres to 42.5 acres. As formation capacity decreases, the additional oil recovered by reducing well spacing increases. At a formation capacity of 53.3 md-ft, decreasing pattern size from 85 acres to 42.5 acres increases waterflood recovery by **3.8% OOIP** (Dirscoll, 1974).

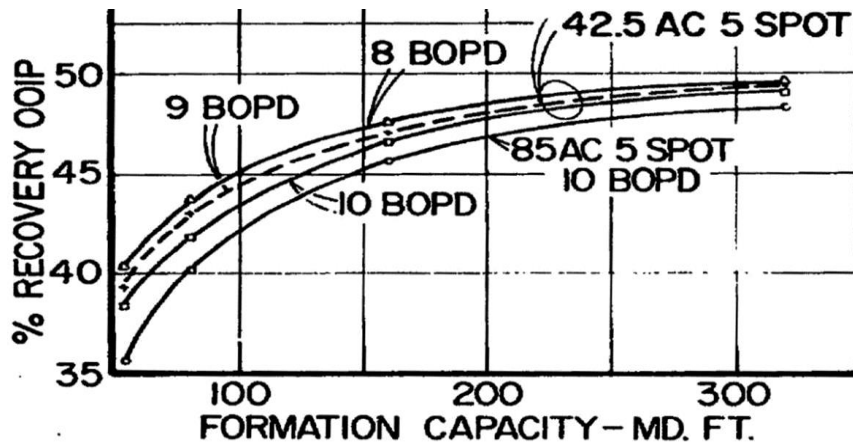


Figure 3.15: The Effect of Formation Capacity on Economic Waterflood Recovery in the Levelland Unit (Dirscoll, 1974).

3.3 SUMMARY

Based on published field data, the improvement in waterflood recovery expected from pattern size reduction ranges from 1% to 22% OOIP. However, the significance of these percentages depends entirely on the amount of OOIP. In the Yates-Queen Sand, a 5.4% improvement in waterflood recovery translated to an additional 14.6 million barrels of oil. Whereas, an improvement in recovery of 9.9% OOIP only corresponded to a gain of 2.4 million barrels of oil in the Grayburg Dolomite.

The dependence of waterflood recovery on pattern size can be attributed to factors such as reservoir geology, “wedge-edge” oil recovery, pattern configuration, communication with water-bearing zones, and economics. Reservoir features that influence infill potential include areal pay-zone discontinuity, preferential flooding directions, and vertical reservoir discontinuity.

Chapter 4: Model Development

In most of the literature presented in Chapter 3, the improvement in ultimate waterflood recovery resulting from pattern size reduction was estimated through decline curve analysis. To more accurately investigate the dependence of oil recovery on flooding pattern size, three-dimensional simulation models were developed using CMG's IMEX. All of the models created for this study share the same: number of grid blocks, grid block dimensions, initial conditions, Pressure-Volume-Temperature (PVT) properties and flow properties. However, each model was created with a unique set of permeability values in order to represent various types of reservoir heterogeneity. Moreover, different well spacing scenarios were created for each reservoir model.

4.1 GRID DEFINITION

A $16 \times 16 \times 16$ Cartesian grid was created for all the models examined in this study. Grid blocks were assigned dimensions of 467 ft in the x and y directions, and 6.25 ft in the z direction. Hence, making the model 100 ft thick with an area of 1,281.7 acres (7,472 ft in the x and y directions). Furthermore, depth to the top of the grid was selected to be 3,000 ft, as illustrated in Figure 4.1 below.

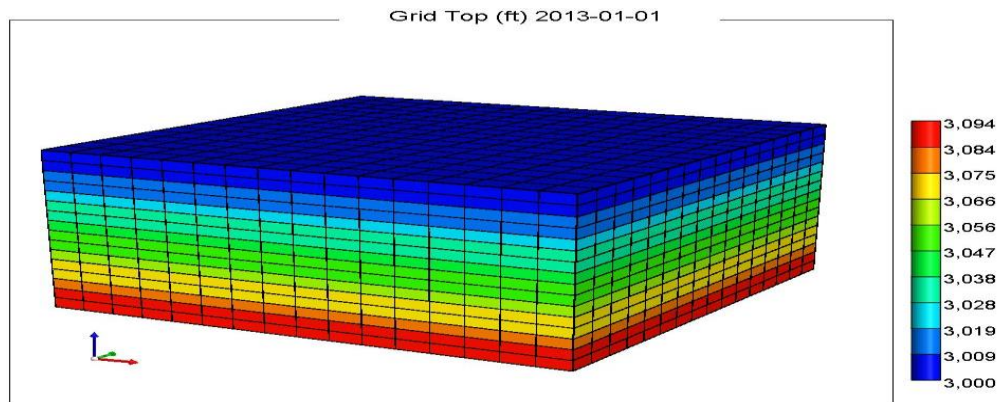


Figure 4.1: Model Grid Top Depths.

4.2 INITIAL CONDITIONS

The initial reservoir pressure was selected to be 1,328 psi at a datum depth of 2,800 ft. With an assigned bubble point pressure of 400 psi, oil in the reservoir is undersaturated. In addition, the oil-water-contact (OWC) was chosen to be 3,300 ft deep. Therefore, making the deepest grid blocks 200 ft shallower than the OWC (Figure 4.1).

4.3 PVT PROPERTIES

A black-oil fluid model was selected for this study. Since most of the fields presented in Chapter 3 had low viscosity crudes, a low oil viscosity of 0.73 cp (at reservoir conditions) was used in this study. Because the reservoir pressure was maintained above the bubble point (P_b) in all the simulations, oil viscosity and compressibility were assumed to be constant. Whereas, the behavior of the oil formation volume factor above the bubble point pressure was controlled by equation (2) below (McCain, 1990). Other fluid properties used in the simulations are in Table 4.1.

Oil Viscosity, μ_o (for $P > P_b$)	0.73 cp
Brine Viscosity, μ_w	1.29 cp
Oil Formation Volume Factor, B_{ob} (at $P = P_b$)	1.181 RB/STB
Water Formation Volume Factor, B_{wi}	1.010 RB/STB
Solution Gas Oil Ratio, R_{so} (for $P > P_b$)	138.27 scf/STB
Oil Compressibility, c_o (for $P > P_b$)	$7.8324 \times 10^{-6} \text{ psi}^{-1}$
Water Compressibility, c_w	$3.0 \times 10^{-6} \text{ psi}^{-1}$
Oil Density, ρ_o (at $P=14.7 \text{ psia}$, $T=60^\circ\text{F}$)	51.79 lb/ft ³
Brine Density, ρ_w (at $P=14.7 \text{ psia}$, $T=60^\circ\text{F}$)	71.95 lb/ft ³

Table 4.1: Fluid Properties.

$$B_o = B_{ob} \text{EXP} [c_o(P_b - P)] \quad (2)$$

4.3 FLOW PROPERTIES

The rock's effective permeability to a certain phase is the result of the product of relative permeability and absolute permeability. The relative permeabilities used in the simulations are in Figure 4.2. As can be observed in Figure 4.2, the reservoir has a connate water saturation of 20% and a residual oil saturation of 39%. Moreover, the reservoir rock is strongly water-wet. Figure 4.3 shows the oil-water drainage capillary pressure curve used for model generation. As previously mentioned, the OWC is 200 ft deeper than the deepest grid blocks, which means that initially, the water saturation is equal to 20% everywhere in the model.

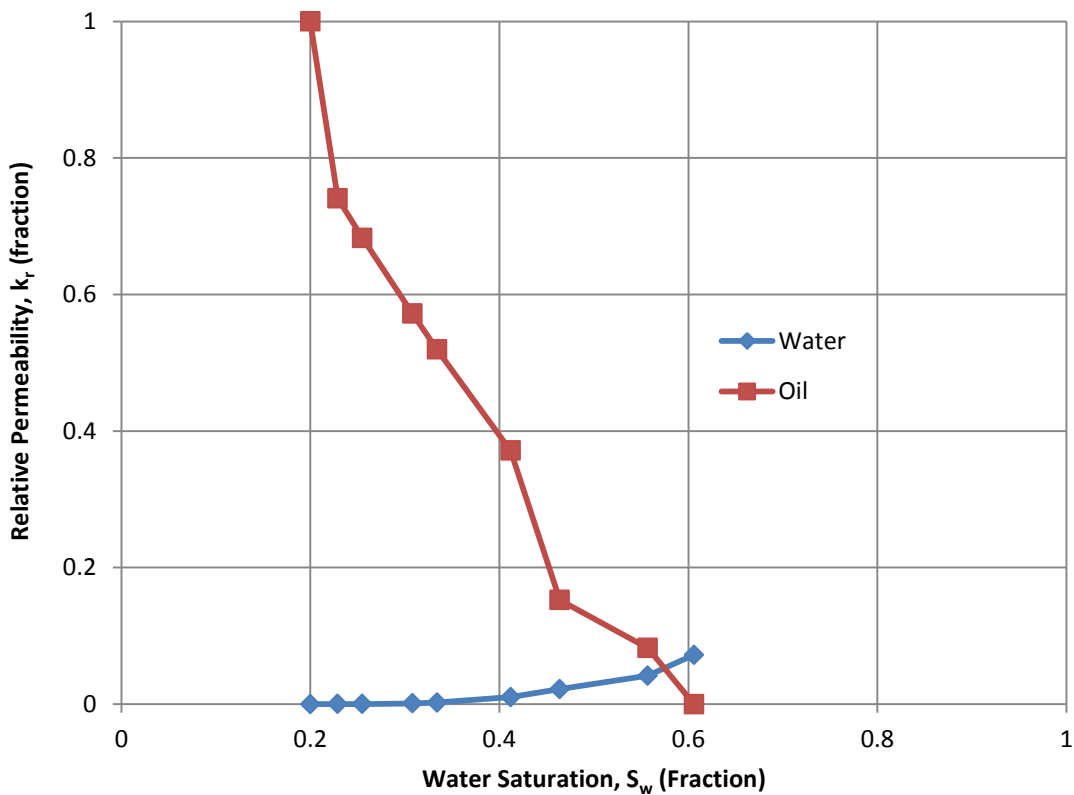


Figure 4.2: Oil-Water Relative Permeability Curves.

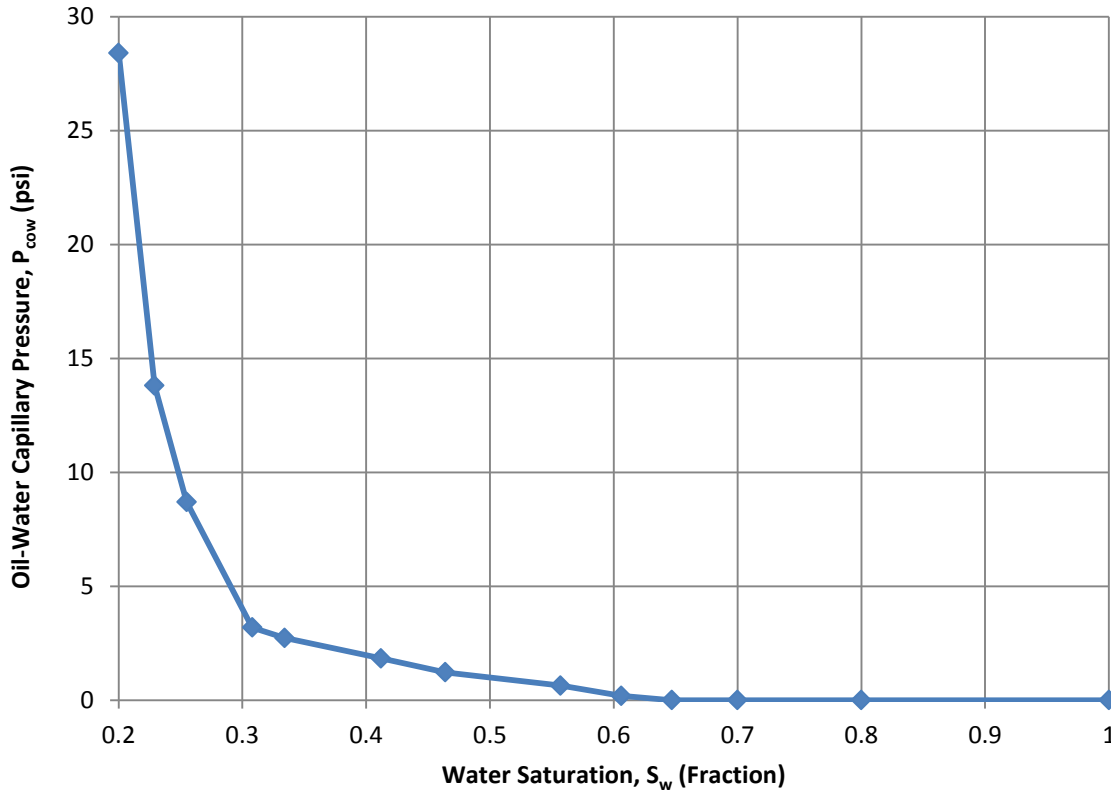


Figure 4.3: Oil-Water Capillary Pressure as a Function of Water Saturation.

4.4 POROSITY AND PERMEABILITY

With the exception of a few models, the initial porosity was set to 18% in the cases created for this study. On the other hand, distinct permeability values were assigned to different grid blocks depending on the type of heterogeneity being modeled. Stochastic permeability fields were generated using a Fast Fourier Transform (FFT) simulator developed by Dr. James W. Jennings (Jennings et al., 2000). Autocorrelation lengths in the x, y and z directions were manipulated to represent different types of reservoirs. Then, equation (3) was used to convert the generated data into lognormal permeability distributions.

$$k(i, j, k) = EXP [\ln(\bar{k}) + stdev(lnk) \times K(i, j, k)] \quad (3)$$

Where,

$k(i,j,k)$ is the lognormal permeability.

$\ln(\bar{k})$ is the mean of the lognormal permeabilities.

$\text{Stdev}(\ln k)$ is the standard deviation of the lognormal permeabilities.

$K(i,j,k)$ is the output of the FFT simulator.

The desired degree of reservoir heterogeneity was then achieved through varying the standard deviation. Furthermore, different types of reservoir heterogeneity were modeled by either assigning zero porosity and permeability values to certain grid blocks or by introducing directional permeability trends.

4.5 VERTICAL WELL PLACEMENT AND CONSTRAINTS

To investigate the impact of pattern size on ultimate waterflood recovery, three development scenarios were considered in this study: 160, 40, and 10 acre five-spots (Table 4.2). Patterns with a producer-to-injector ratio of one are the most frequently used patterns in the industry (Gulick and McCain, 1998). Hence, the selection of five-spots for this study.

Triplicates were made of each reservoir model, all of which were developed with a different pattern size (Figures 4.4-4.6). The well locations are indicated with grey labels: where “Inj-” and “Oil-” represent injectors and producers, respectively. In all the modeled cases, both injection and production wells were perforated across all 16 grid blocks in the z direction. Moreover, all the wells were online (producing/injecting) from the initial simulation start time. Additionally, injectors and producers were only allowed to operate within well-defined constraints.

Injection wells were allowed to inject up to 3,000 barrels of water per day (BWPD) as long as the original reservoir pressure of approximately 1,380 psi was maintained throughout the simulations. On the other hand, each production well was assigned maximum rate of 10,000 BOPD. Producers were shut-in whenever the bottom-hole pressure fell below the bubble point pressure, or oil rate dropped below 10 BOPD, or watercut exceeded 95%. The simulation runs would only terminate once the total production rate dropped to zero.

Five-Spot Patterns					
Pattern Size (Acres)	Well Spacing (Acres)	Number of Producers	Number of Injectors	Total Number of Wells	Abandonment Rate (Barrels of Oil)
160	80	13	12	25	130
40	20	32	32	64	320
10	5	128	128	256	1,280

Table 4.2: The Development Scenarios Used in the Simulations

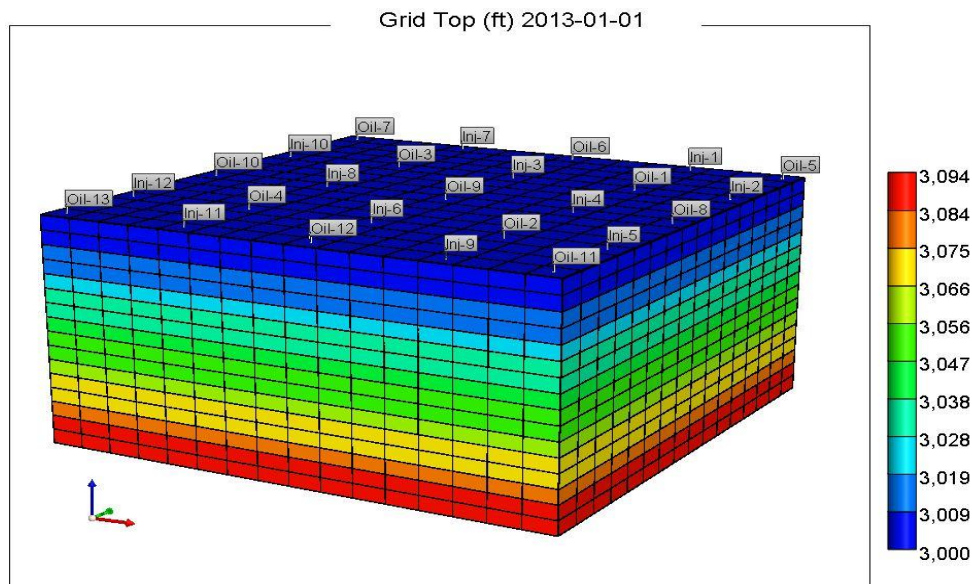


Figure 4.4: 160 Acre Five-Spot Development Scenario.

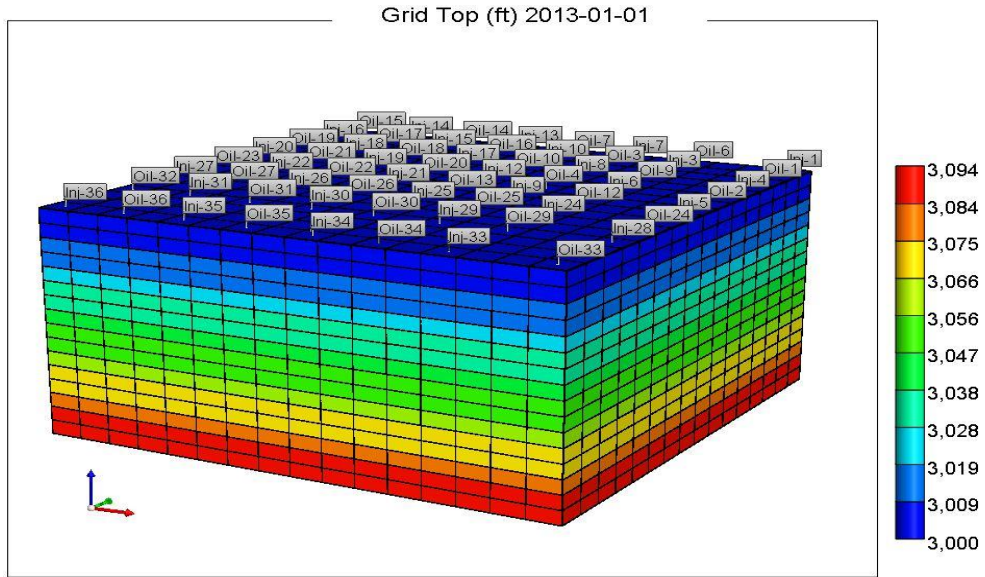


Figure 4.5: 40 Acre Five-Spot Development Scenario.

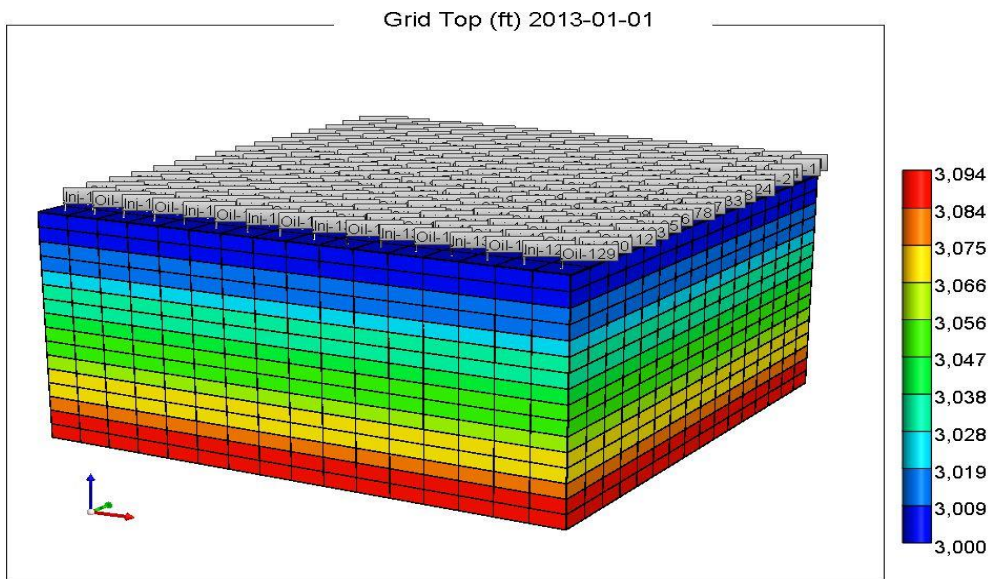


Figure 4.6: 10 Acre Five-Spot Development Scenario.

Chapter 5: Simulation Results and Discussion

To test the validity of the concepts presented in section 3.2, numerous simulation runs were conducted on different reservoir models. These models include both homogeneous and heterogeneous cases. The types of heterogeneities considered include reservoirs with highly-variable permeabilities, reservoirs with preferential flooding orientations, areally discontinuous reservoirs, and vertically discontinuous (layered) reservoirs. For the purpose of this study, recovery efficiency is defined as the cumulative oil produced at simulation termination ($N_{p|q=0}$) expressed as a percentage of OOIP.

5.1 HOMOGENEOUS CASES

5.1.1 Regular Patterns

A plethora of simulation runs were completed on homogeneous reservoirs with a wide range of permeability values. In all of these runs, waterflood recovery was found to be independent of development pattern size. Figure 5.1 illustrates the cumulative oil produced over a period of time from a reservoir with a constant permeability of 50 md. Although no improvement in ultimate recovery efficiency was realized, oil recovery was significantly accelerated by reducing the pattern size from 160 to 10 acres (Table 5.1). Because of the time value of money, this acceleration in production has substantial economic implications. For cases developed with wider well spacing, oil could be left behind at an economic limit rate.

Pattern Size (Acres)	Recovery Efficiency (%)	Recovery Time (Years)
160	50.88	150
40	50.83	88
10	50.62	7

Table 5.1: Simulation Results for a 50 md Homogeneous Reservoir.

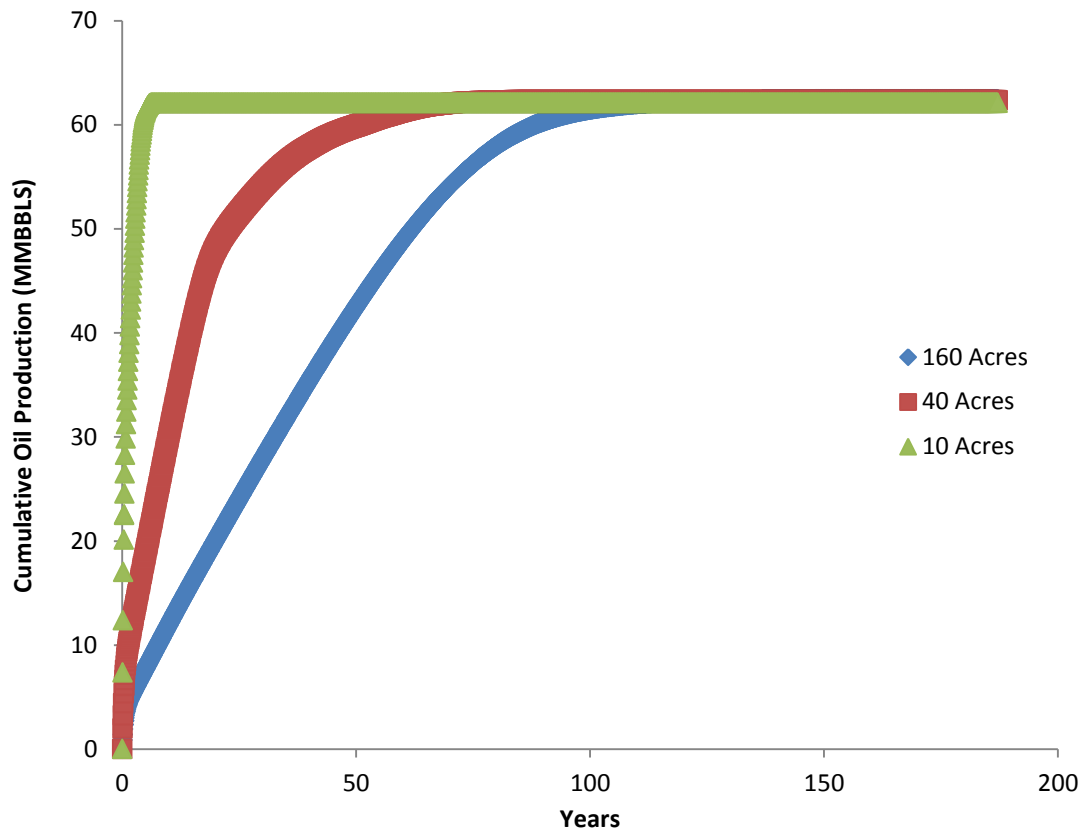


Figure 5.1: Cumulative Oil Production as a Function of Time for a 50 md Homogeneous Reservoir Developed with Five-Spot Patterns of Different Sizes.

5.1.2 Irregular Patterns

Similarly, pattern size reduction had little influence on ultimate recovery efficiency in models developed with irregularly shaped patterns. Figure 5.2 shows a 10 md homogeneous reservoir model populated with chickenwire patterns. As demonstrated in Figure 5.3, 6 infill production wells were added to these patterns in the locations proposed by Thomas and Driscoll (1973). While Thomas and Driscoll (1973) reported that a 3.6% improvement in waterflood recovery was achieved through such infills, simulation results only indicated a 0.31% (451,680 BBLs) improvement in recovery efficiency was attained by the additional production wells. This discrepancy is mainly

because recovery efficiency was defined differently in this study than in the report published by Thomas and Driscoll (1973). Their study defined recovery efficiency as the amount of oil recovered at the economic limit. Despite only having little impact on recovery efficiency, the additional production wells did manage to accelerate ultimate oil recovery by 77 years.

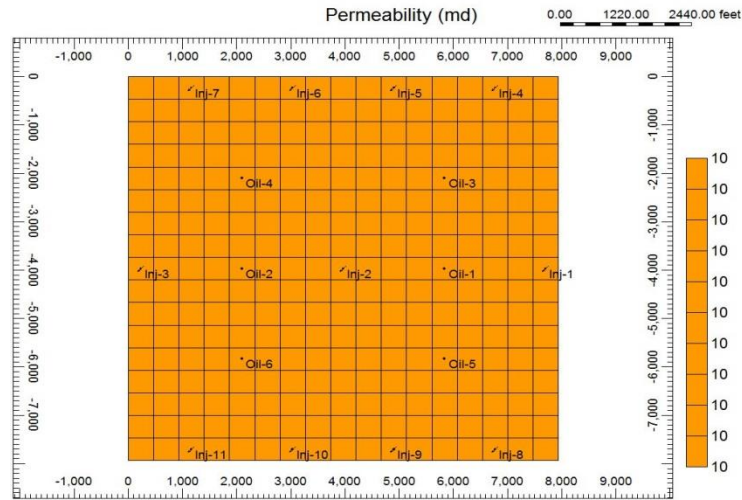


Figure 5.2: Top View of a 10 md Homogeneous Three-Dimensional Reservoir Model Developed with Chickenwire Patterns.

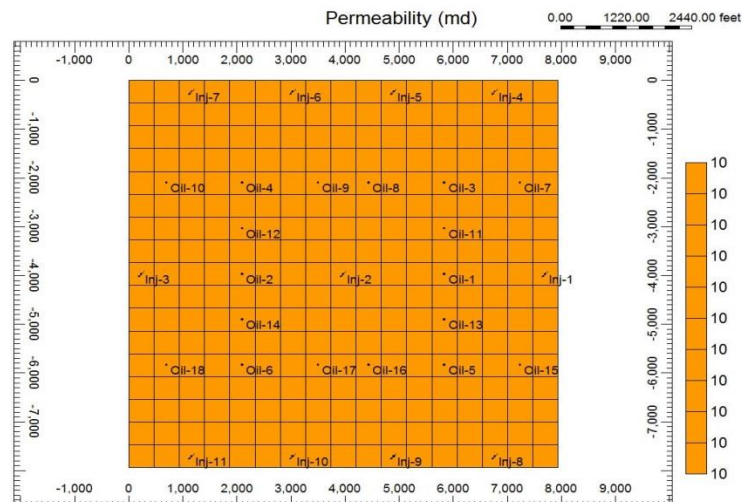


Figure 5.3: Top View of a 10 md Homogeneous Three-Dimensional Reservoir Model Developed with Chickenwire Patterns and Infill Wells.

5.2 HETEROGENEOUS CASES

5.2.1 Reservoirs with Highly-Variable Non-Zero Permeabilities

Several models were generated for reservoirs with a wide range of permeability values. These reservoir models were assigned a standard deviation of 1, Dykstra-Parsons coefficients (V_{DP}) ranging from 0.61-0.67, and a variety of autocorrelation lengths in the x, y, and z directions. Irrespective of the selected autocorrelation lengths, similar results were observed in models sharing the same average permeability.

Figure 5.4 illustrates the permeability distribution in a spatially uncorrelated reservoir model with an average permeability of 50 md. As shown in Figure 5.4, permeability values range from 1 md to 4 Darcies. Examples of other reservoir models with different autocorrelation lengths are shown in Figures 5.5 and 5.6. Simulations on reservoirs with highly-variable non-zero permeabilities provided similar results to those obtained from homogeneous cases; pattern size reduction accelerated production but had little impact on ultimate waterflood recovery (Table 5.2).

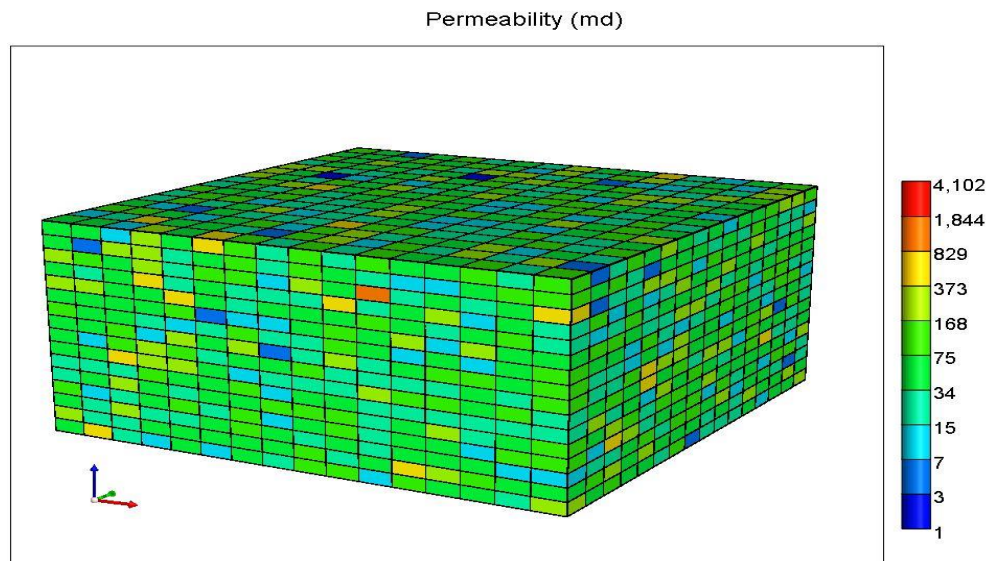


Figure 5.4: Permeability Distribution in a Spatially Uncorrelated Reservoir Model with an Average Permeability of 50 md.

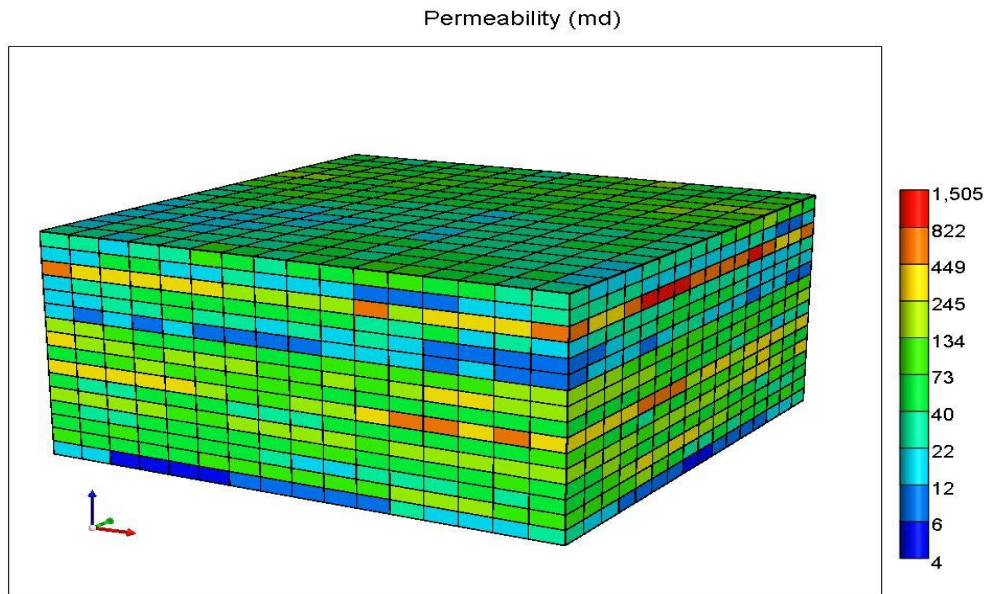


Figure 5.5: Permeability Distribution in a Reservoir Model with an Average Permeability of 50 md and Autocorrelation Lengths of 7,472 ft in the x and y Directions.

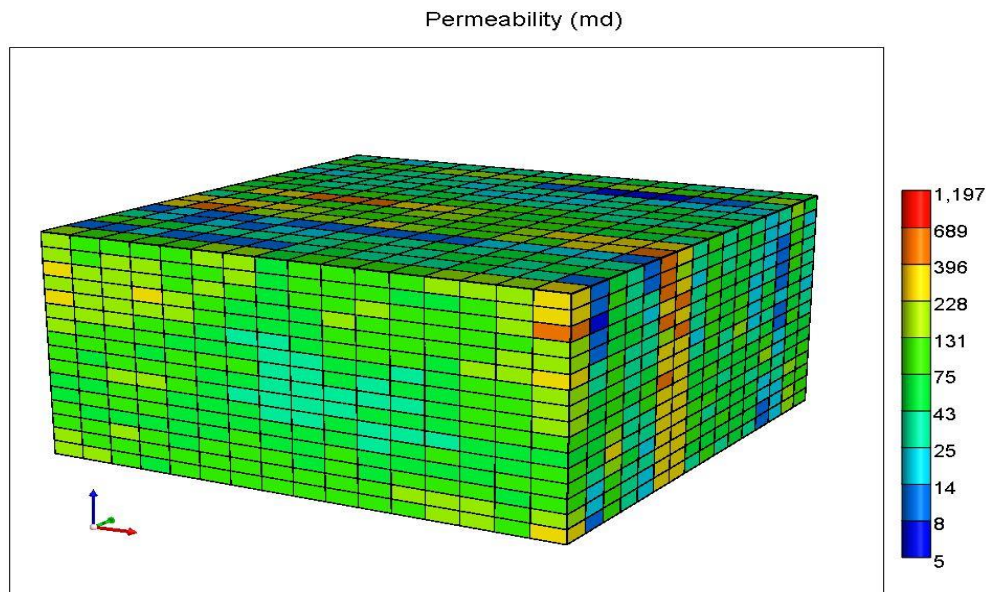


Figure 5.6: Permeability Distribution in a Reservoir Model with an Average Permeability of 50 md and Autocorrelation Lengths of 7,472 ft in the x and z Directions.

Autocorrelation Length (ft)			Pattern Size (Acres)	Recovery Efficiency (%)	Recovery Time (Years)
x	y	z			
1	1	1	160	50.80	132
			40	50.58	64
			10	50.23	8
7,472	7,472	1	160	50.54	77
			40	50.39	51
			10	50.17	2
7,472	1	7,472	160	50.77	199
			40	50.68	99
			10	50.46	13
3,736	3,736	10	160	50.38	93
			40	50.19	61
			10	50.03	2
1,868	1,868	10	160	50.53	120
			40	50.31	59
			10	50.14	8
934	934	100	160	50.73	150
			40	50.71	83
			10	50.49	14

Table 5.2: Simulation Results for Reservoirs with Highly-Variable Permeabilities and an Average Permeability of 50 md.

5.2.2 Reservoirs with Preferential Flooding Orientations

In all the above-mentioned reservoir models, permeability within each grid block was assumed to be isotropic. Logically, increasing areal permeability anisotropy (k_x/k_y) would result in reservoirs with favorable flooding directions. One example of such reservoirs is shown in Figures 5.7 and 5.8. While the x and z directions were assigned average permeabilities of 1 Darcy (Figure 5.7), average permeability in the y direction was selected to be 5 md (Figure 5.8). Hence, making the anisotropy ratio (k_x/k_y) =200.

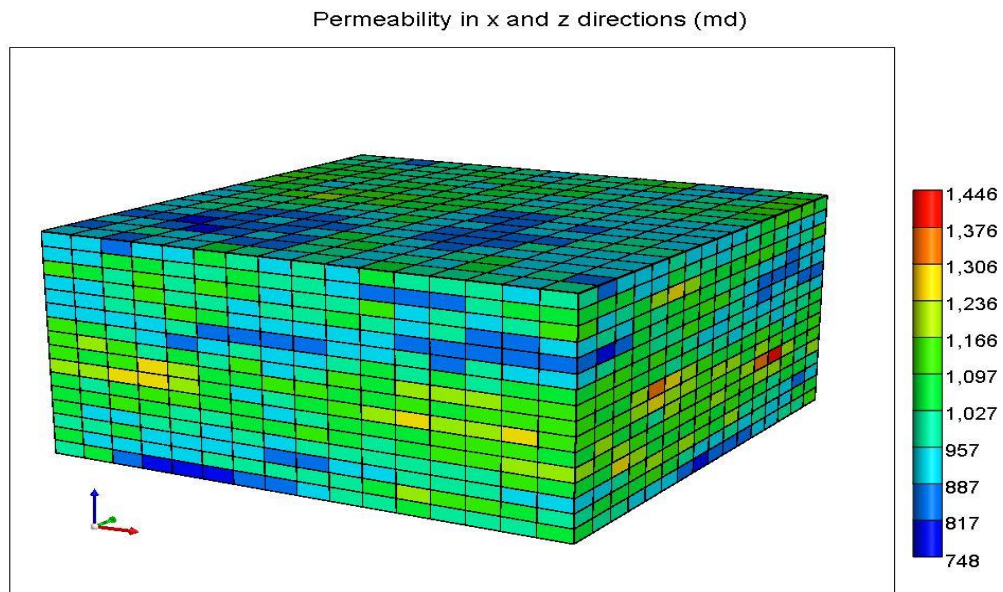


Figure 5.7: Permeability in the x and z Directions for an Anisotropic Reservoir Model ($k_{avg} = 1,000$ md).

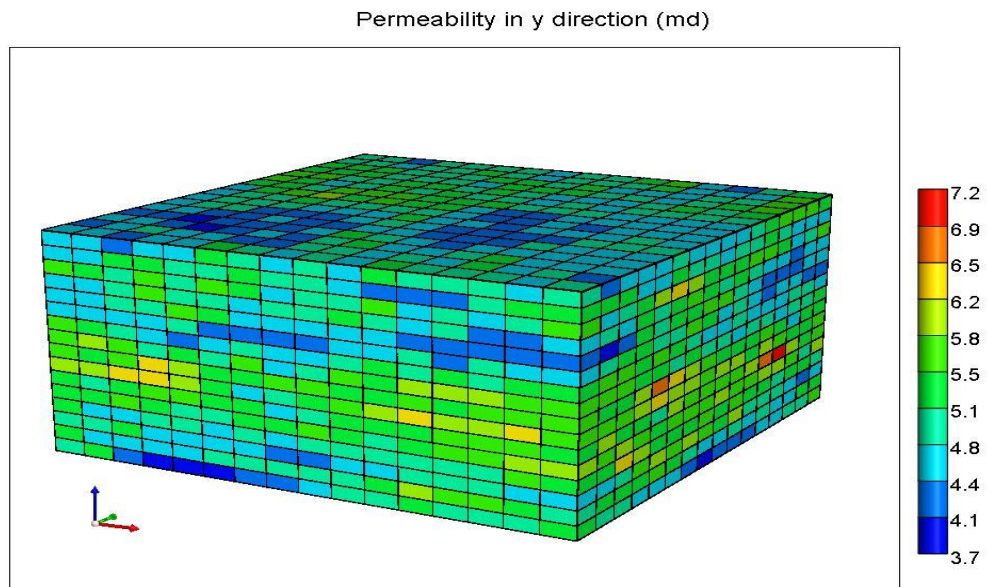


Figure 5.8: Permeability in the y Direction for an Anisotropic Reservoir Model ($k_{avg} = 5$ md).

In this particular model, simulation results indicate that the areal sweep efficiency is highly dependent on bottom-hole injection pressure (Figure 5.9). At low injection pressures, ultimate waterflood recovery was found to be almost identical regardless of pattern size. However, as injection pressures were increased, lower oil recoveries were realized from models developed with wider spaced patterns. The high injection pressures displayed in Figure 5.9 are not uncommon, especially when operators aim to accelerate oil production.

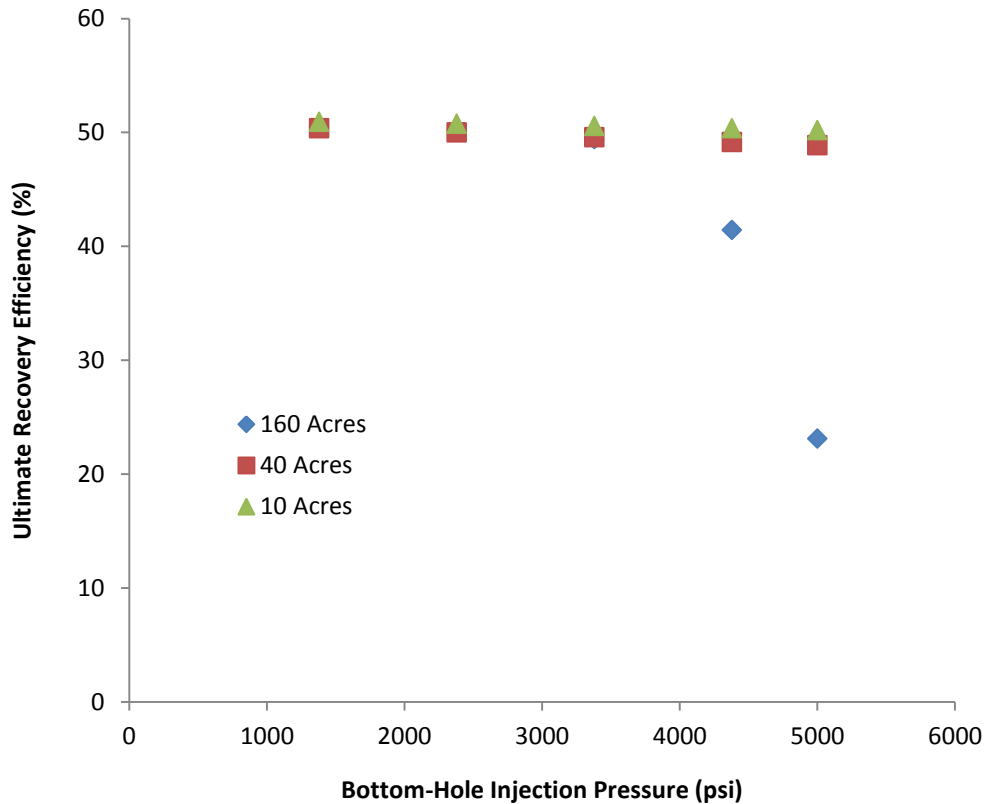


Figure 5.9: Recovery Efficiency as a Function of Bottom-Hole Injection Pressure for an Anisotropic Reservoir Model ($k_x/k_y=200$) Developed with Five-Spot Patterns of Different Sizes.

High bottom-hole injection pressures caused by over injection can result in the bypassing of significant oil quantities because of premature water encroachment. This concept is illustrated in Figure 5.10, where warm colors represent the remaining oil saturation at simulation termination. The reduction of pattern size increased ultimate waterflood recovery by improving areal sweep (Figures 5.11 and 5.12). For an injection pressure of 5000 psi, a plot of oil production rates versus cumulative oil production for different development scenarios is presented in Figure 5.13.

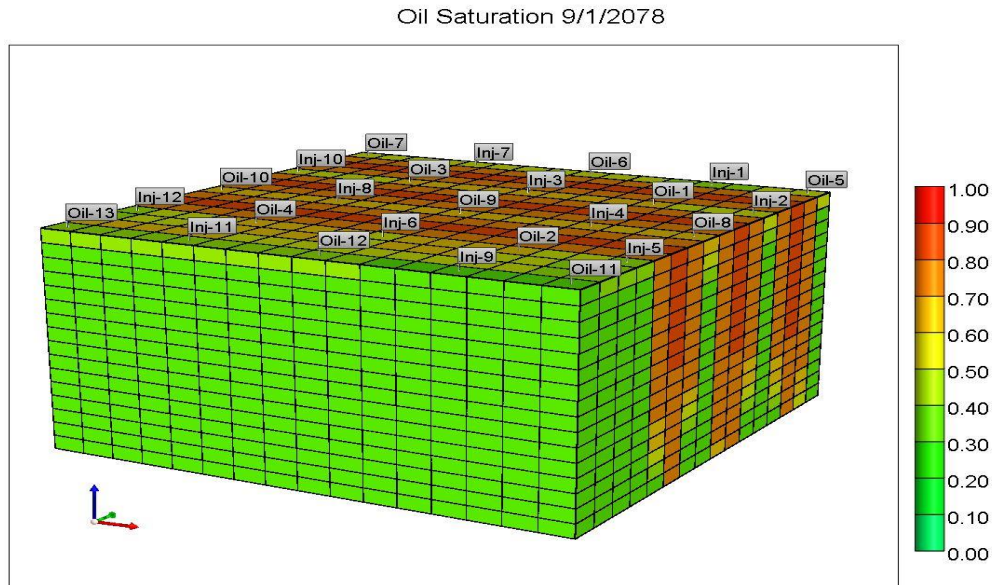


Figure 5.10: Oil Saturation at Simulation Termination for an Anisotropic Reservoir ($k_x/k_y=200$) Developed with 160 Acre Five-Spot Patterns (Bottom-Hole Injection Pressure = 5,000 psi).

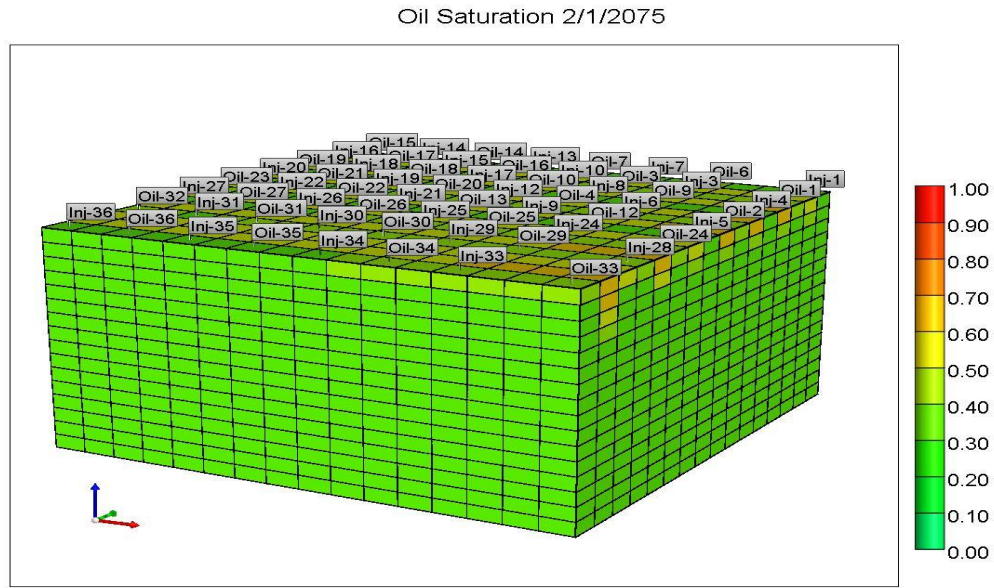


Figure 5.11: Oil Saturation at Simulation Termination for an Anisotropic Reservoir ($k_x/k_y=200$) Developed with 40 Acre Five-Spot Patterns (Bottom-Hole Injection Pressure = 5,000 psi).

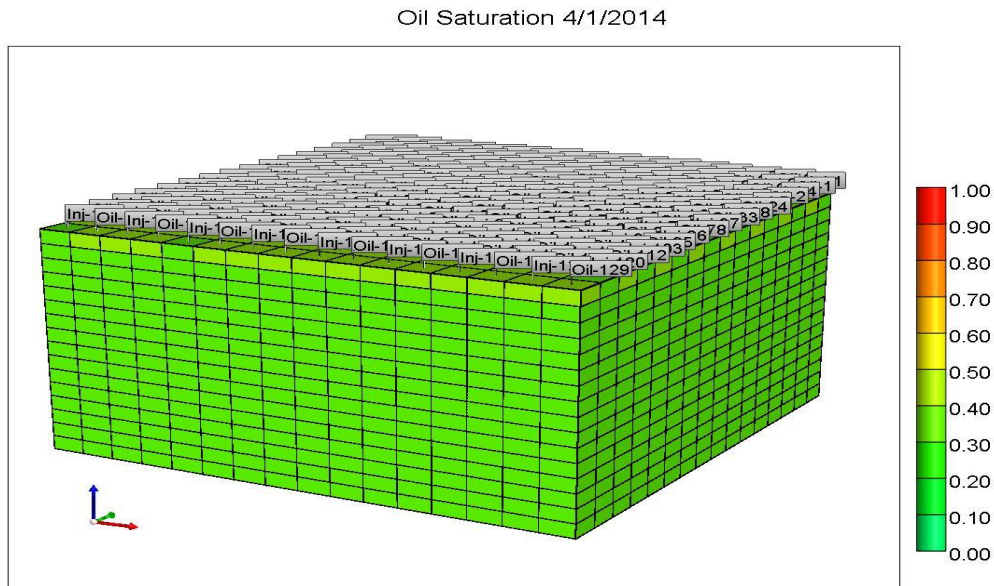


Figure 5.12: Oil Saturation at Simulation Termination for an Anisotropic Reservoir ($k_x/k_y=200$) Developed with 10 Acre Five-Spot Patterns (Bottom-Hole Injection Pressure = 5,000 psi).

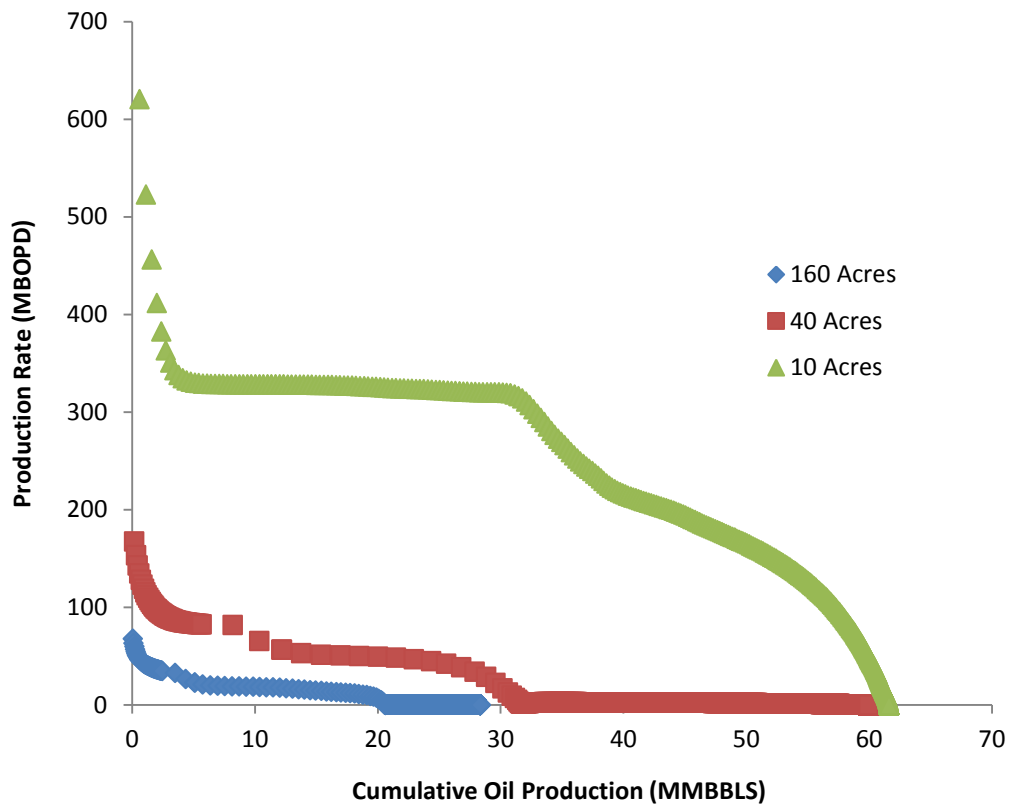


Figure 5.13: Daily Oil Production Rate as a Function of Cumulative Oil Production for an Anisotropic Reservoir ($k_x/k_y=200$) Developed with Five-Spot Patterns of Different Sizes (Bottom-Hole Injection Pressure = 5,000 psi).

In Figure 5.13, similar production behaviors are exhibited in all three curves. Initially, oil production rates start off high. They then rapidly drop and plateau at a sustainable production rate. Finally, watercut begins to rise and oil rates continuously decline until the producers are shut-in. Smaller pattern sizes have higher plateau rates, which result in larger quantities of cumulative oil production.

Results indicate that a 111% improvement in recovery efficiency (31.587 million barrels of oil) was achieved through decreasing the pattern size from 160 acres to 40 acres. Further reduction of the development pattern size from 40 acres to 10 acres led to the recovery of an additional 1.615 million barrels of oil. Not only did reducing the

pattern size from 160 to 10 acres increase cumulative ultimate oil production, it also accelerated recovery by approximately 64 years.

Similar simulations were conducted on models with less permeability anisotropy. For models with $k_x/k_y \leq 10$, results suggested that pattern size had no impact on waterflood recovery. Hence, making it apparent that favorable flooding directions that affect waterflood recovery are more likely to arise because of the presence of open fractures than because of stratigraphy-related anisotropy.

5.2.3 Areally Discontinuous Reservoirs

As previously mentioned, areal reservoir discontinuity is the most likely explanation for the dependence of waterflood recovery on pattern size. In this study, areally discontinuous reservoir models were generated by imbedding non-porous impermeable blocks into the grid. Beginning with a 50 md spatially uncorrelated reservoir model (Figure 5.4), grid blocks with permeability values below a certain cutoff were assigned zero porosities and zero permeabilities. Then, the desired degree of reservoir discontinuity was achieved through manipulating the permeability cutoff point. This strategy was employed in creating nine different reservoir models, each with a different percentage of non-porous impermeable grid blocks.

Figure 5.14 demonstrates the recovery efficiency associated with different development scenarios for models with interspersed zero-porosity and zero-permeability grid blocks. In the absence of non-porous impermeable grid blocks, an ultimate recovery efficiency of 50% was obtained from all three pattern sizes. Regardless of well spacing, similar ultimate recovery efficiencies were achieved as long as a continuous path of permeable grid blocks existed between production and injection wells. Since fluid flow is controlled by the medium, sweep efficiency in such models is considered a percolation

process. For the whole grid (simple cubic lattice), the site percolation threshold of permeable grid blocks is 31% (Bryant, 2012). This threshold indicates that more than 69% of the grid blocks must be assigned zero permeability values to prevent percolation across the grid. However, compartmentalization does occur at a lower percentage of impermeable grid blocks. Hence, the improvement in waterflood recovery from pattern size reduction observed in models where the percentage of zero permeability grid blocks is as low as 30.1% (Figure 5.14). A close examination of one of these areally discontinuous reservoir models allows for better visualization of the influence of pattern size on recovery efficiency.

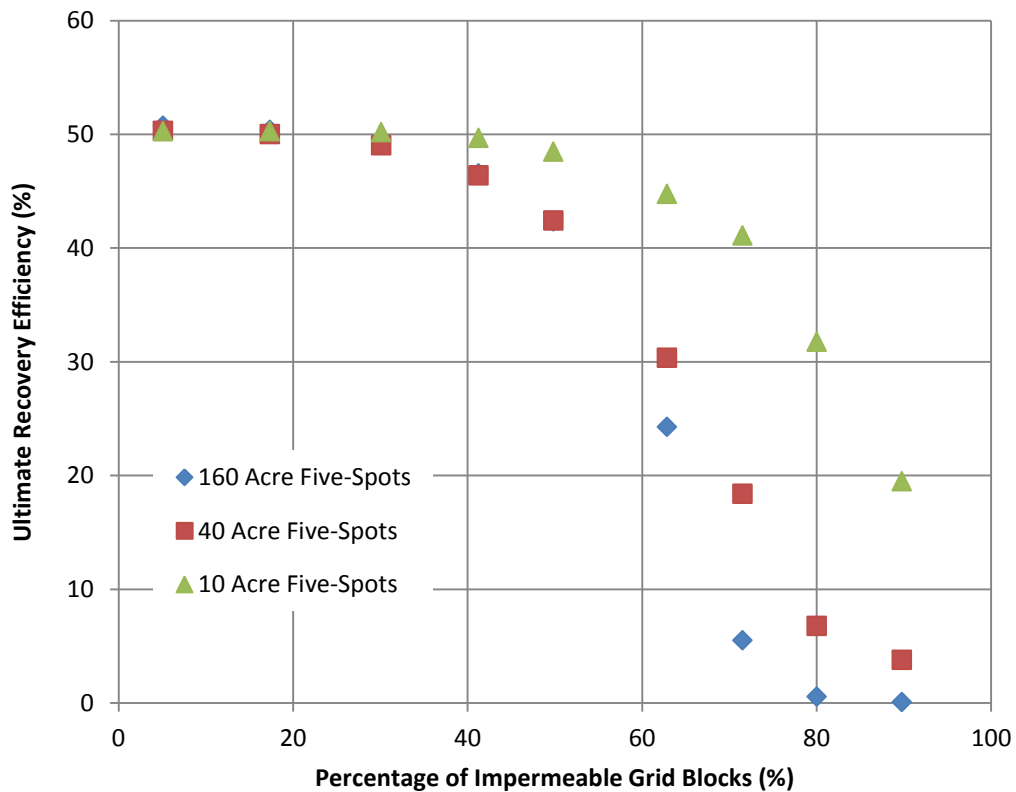


Figure 5.14: Recovery Efficiency as a Function of the Percentage of Non-Porous Impermeable Grid Blocks.

Figure 5.15 shows the permeability distribution of a spatially uncorrelated reservoir model, where 62.87% of the grid blocks were assigned zero porosities and zero permeabilities. For the 160 acre development scenario, ultimate waterflood recovery was found to be 24.27%. This low recovery efficiency is caused by certain pay zones being uncontacted, and others being exclusively contacted by either a producer or an injector. Because of the lack of pressures support from injectors, grid blocks solely contacted by production wells were only partially drained. Moreover, grid blocks only penetrated by injectors were completely unswept.

Figure 5.16 illustrates how certain grid blocks are unswept with 160 acre five-spot patterns. Reducing the pattern size to 40 acres decreased the number of unswept grid blocks (Figure 5.17), therefore increasing ultimate waterflood recovery to 30.35%. Further reduction of the pattern size to 10 acres ensured that all the grid blocks were contacted by wells, which increased ultimate recovery efficiency to 44.75% (Figure 5.18). For the 10 acre development scenario, unswept grid blocks were those exclusively contacted by injection wells.

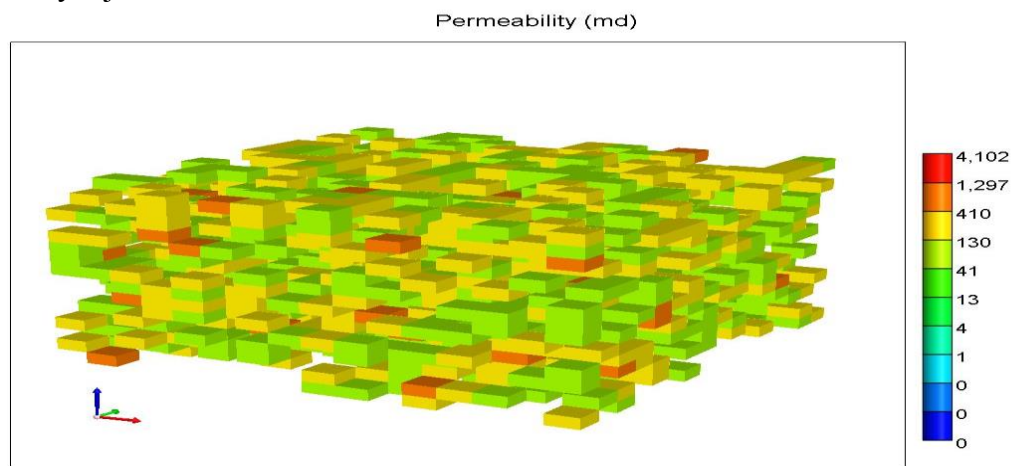


Figure 5.15: Permeability Distribution in a Spatially Uncorrelated Reservoir Model with 62.87% Non-Porous Impermeable Grid Blocks (Legend Colors in Logarithmic Scale).

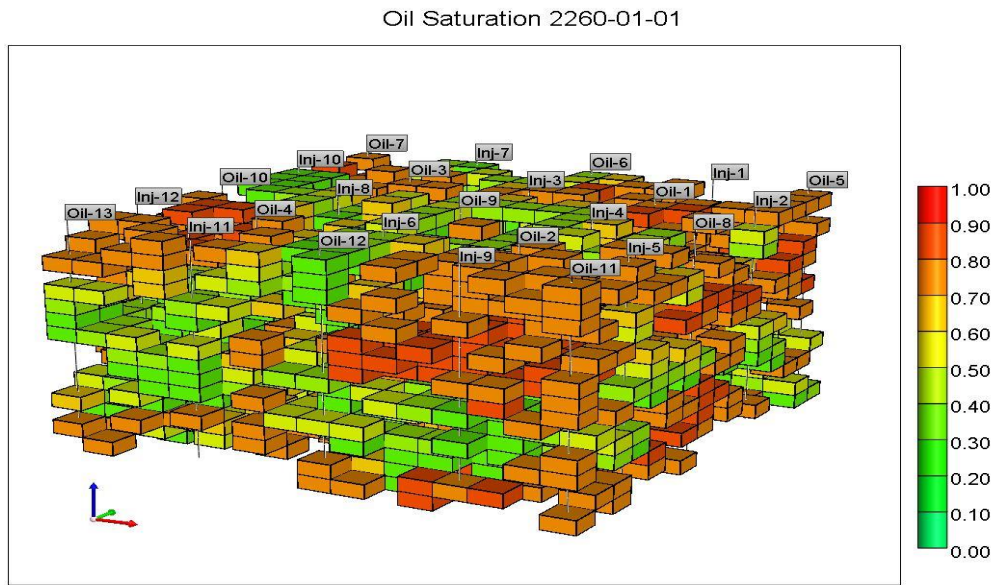


Figure 5.16: Oil Saturation at Simulation Termination for an Areally Discontinuous Reservoir (62.87% Non-Porous Impermeable Grid Blocks) Developed with 160 Acre Five-Spot Patterns.

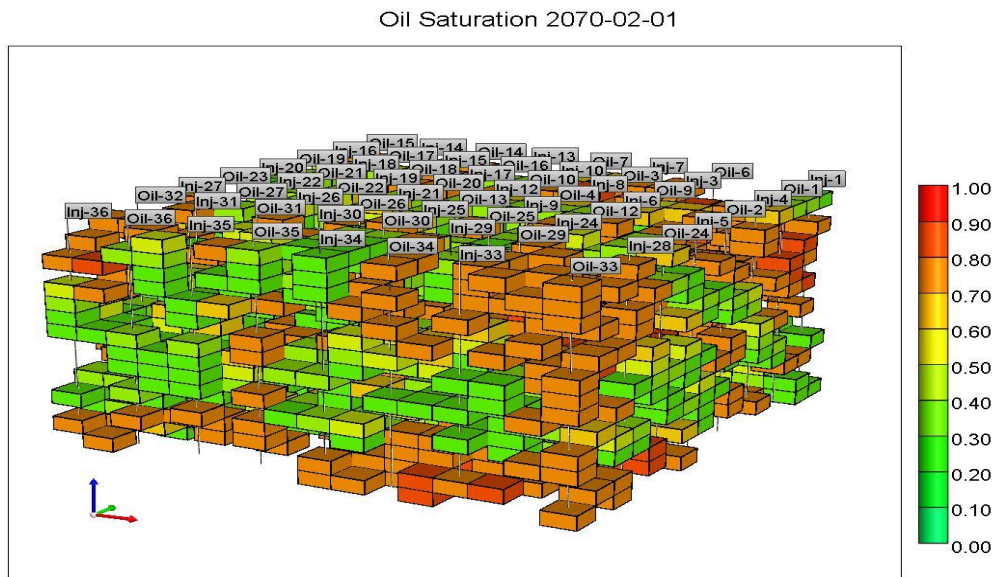


Figure 5.17: Oil Saturation at Simulation Termination for an Areally Discontinuous Reservoir (62.87% Non-Porous Impermeable Grid Blocks) Developed with 40 Acre Five-Spot Patterns.

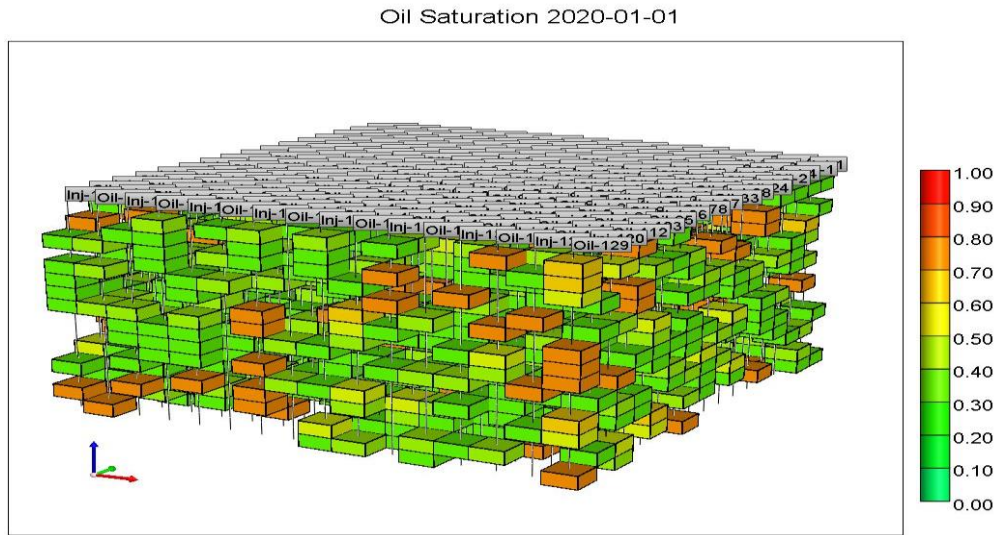


Figure 5.18: Oil Saturation at Simulation Termination for an Areally Discontinuous Reservoir (62.87% Non-Porous Impermeable Grid Blocks) Developed with 10 Acre Five-Spot Patterns.

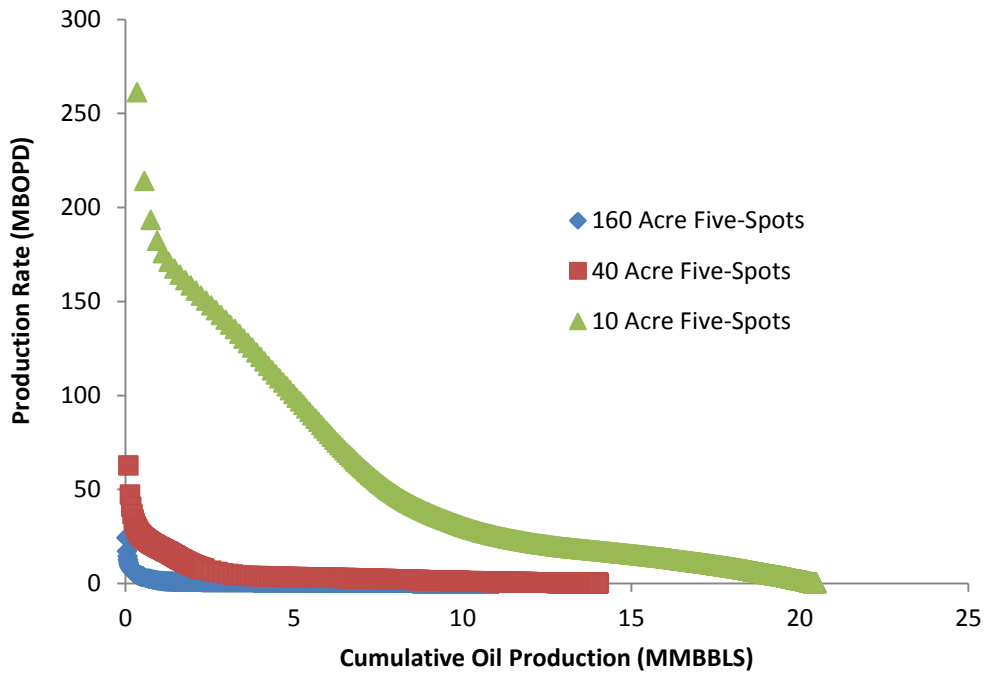


Figure 5.19: Daily Oil Production Rate as a Function of Cumulative Oil Production for an Areally Discontinuous Reservoir (62.87% Non-Porous Impermeable Grid Blocks).

A quantitative illustration of the dependence of ultimate oil recovery on development pattern size is in Figure 5.19. All three curves demonstrate a production behavior similar to that of primary recovery. Oil production rates initially started off high. Then, productivity continuously dropped until the production wells were shut-in. Initial production rates were higher for tighter patterns than they were for larger patterns. Consequently, the cumulative oil produced at simulation termination was inversely related to pattern size.

While the cumulative oil production from 160 acre five-spots was 11.06 million barrels, ultimate oil recoveries of 14.02 million barrels and 20.48 million barrels were achieved by 40 acre five-spots and 10 acre five-spots, respectively. Improvements in recovery of 2.96 million barrels and 9.42 million barrels were achieved by reducing the pattern size to 40 acres and 10 acres, respectively. Such results, along with the diminished recovery time associated with tighter patterns, are what make pattern size reduction an attractive strategy for developing areally discontinuous reservoirs.

5.2.4 Layered Reservoirs

The creation of vertically discontinuous reservoir models required the generation of permeability fields for several layers. These layers were assigned a common uniform thickness of 12.5 ft and autocorrelation lengths of $1,868 \times 1,868 \times 10$ ft. However, a different average permeability was designated for each layer. For the model depicted in Figure 5.20, the average permeability was selected to be 1 md in the top two layers, and 100 md in the bottom two.

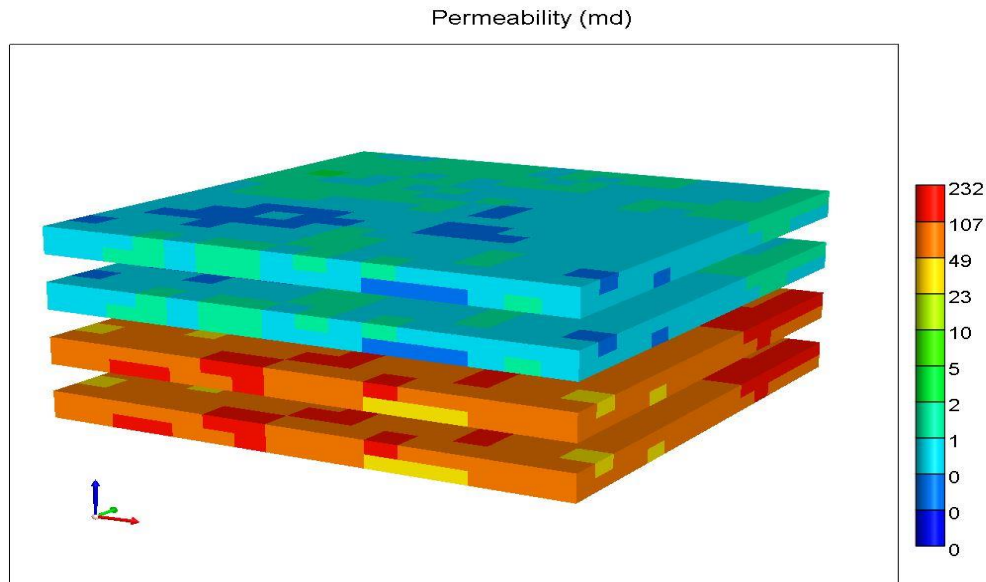


Figure 5.20: Permeability Distribution for a Vertically Discontinuous Reservoir (k_{avg} of Top Two Layers = 1 md, k_{avg} of Bottom Two Layers = 100 md).

Simulations conducted on this reservoir model indicate that ultimate recovery efficiency is inversely related to pattern size. The remaining oil saturation at simulation termination for each development scenario is illustrated in Figures 5.21-5.23. For all three pattern sizes, the bottom two layers were completely swept. On the other hand, significant quantities of oil were left behind in the top two layers. Reducing the pattern size was found to have increased oil recovery from these low permeability layers.

The overall ultimate recovery efficiencies associated with the different development scenarios are in Table 5.3. Decreasing the pattern size from 160 to 40 acres resulted in a 1.52 million barrel (2.47% OOIP) improvement in ultimate oil recovery. Whereas, further reduction of the pattern size from 40 to 10 acres increased ultimate oil recovery by 888,000 barrels (1.45% OOIP).

Unlike in the previous reservoir models, the recovery time of the 40 acre five-spots was actually longer than that of the 160 acre five-spots. The reason behind pattern

size reduction not accelerating recovery in this case is related to vertical sweep. While the smaller patterns did manage to partially drain the low permeability layers, the 160 acre five-spots did not. This conclusion is supported by the slope behavior of production data.

Irregular changes in the slope of the cumulative production data for 40 and 10 acre five-spots are circled in Figure 5.24. Such slope changes are a production characteristic of vertically discontinuous reservoirs with contrasting permeabilities. The absence of this slope behavior from the 160 acre production data indicates that the low permeability layers were completely unswept with 160 acre five-spots.

Pattern Size (Acres)	Recovery Efficiency (%)	Recovery Time (Years)
160	27.08	124
40	29.55	243
10	31.00	47

Table 5.3: Simulation Results for a Three-Dimensional Vertically Discontinuous Reservoir Model Reservoir (k_{avg} of Top Two Layers = 1 md, k_{avg} of Bottom Two Layers = 100 md).

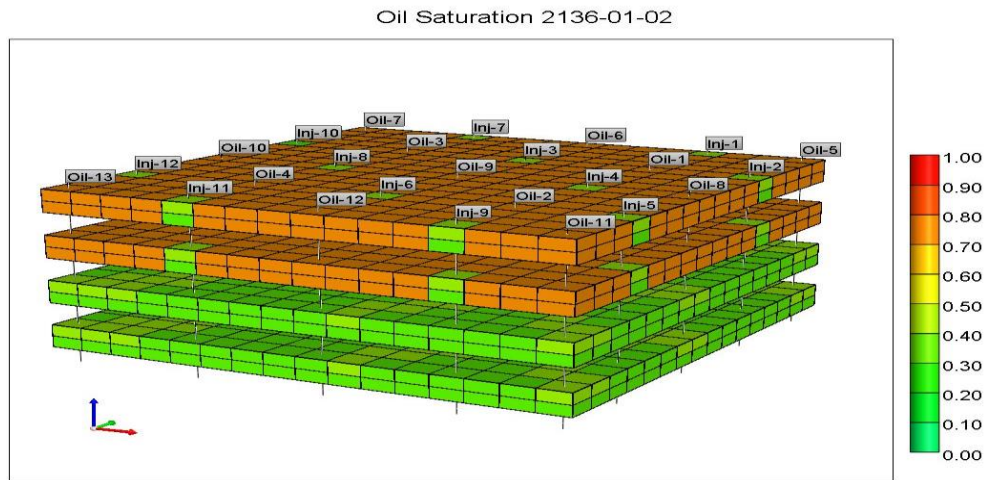


Figure 5.21: Oil Saturation at Simulation Termination for a Vertically Discontinuous Reservoir Developed with 160 Acre Five-Spots (k_{avg} of Top Two Layers = 1 md, k_{avg} of Bottom Two Layers = 100 md).

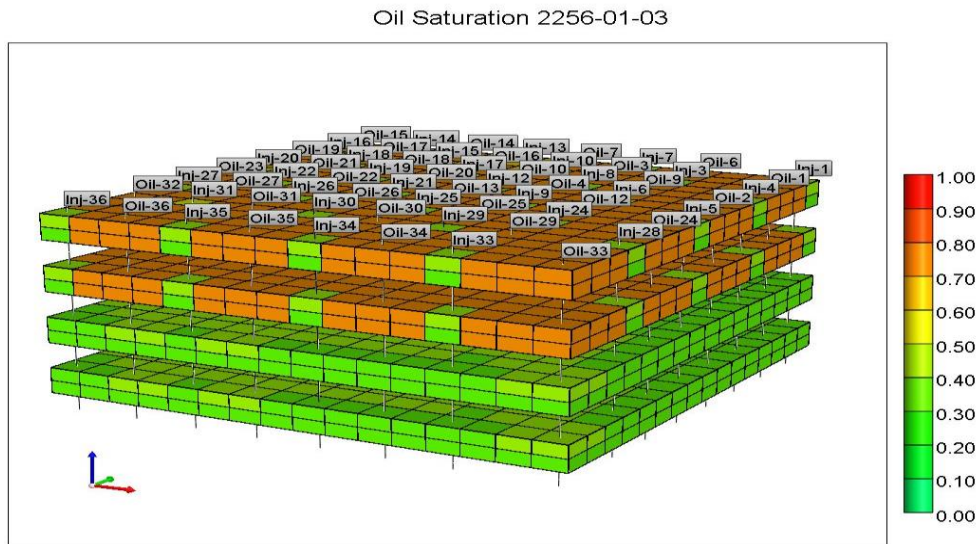


Figure 5.22: Oil Saturation at Simulation Termination for a Vertically Discontinuous Reservoir Developed with 40 Acre Five-Spots (k_{avg} of Top Two Layers = 1 md, k_{avg} of Bottom Two Layers = 100 md).

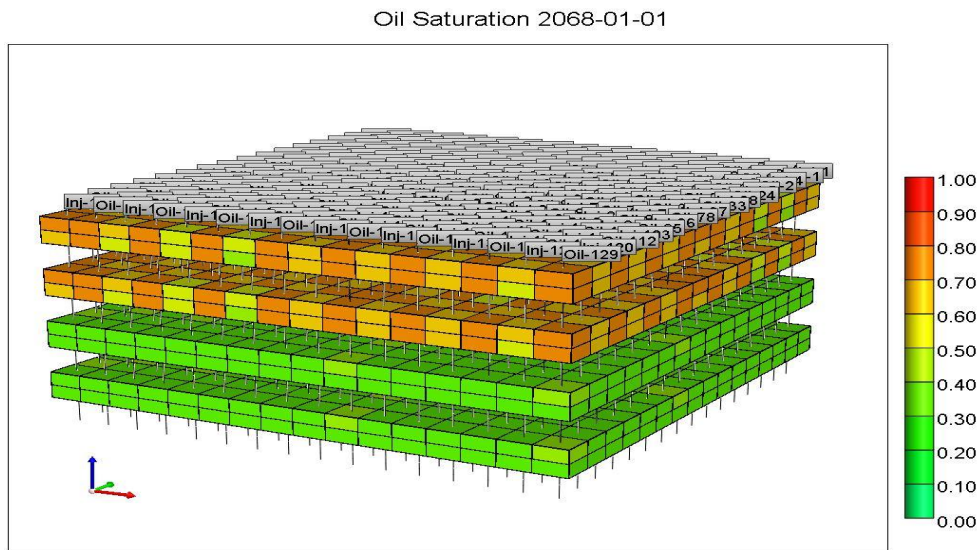


Figure 5.23: Oil Saturation at Simulation Termination for a Vertically Discontinuous Reservoir Developed with 10 Acre Five-Spots (k_{avg} of Top Two Layers = 1 md, k_{avg} of Bottom Two Layers = 100 md).

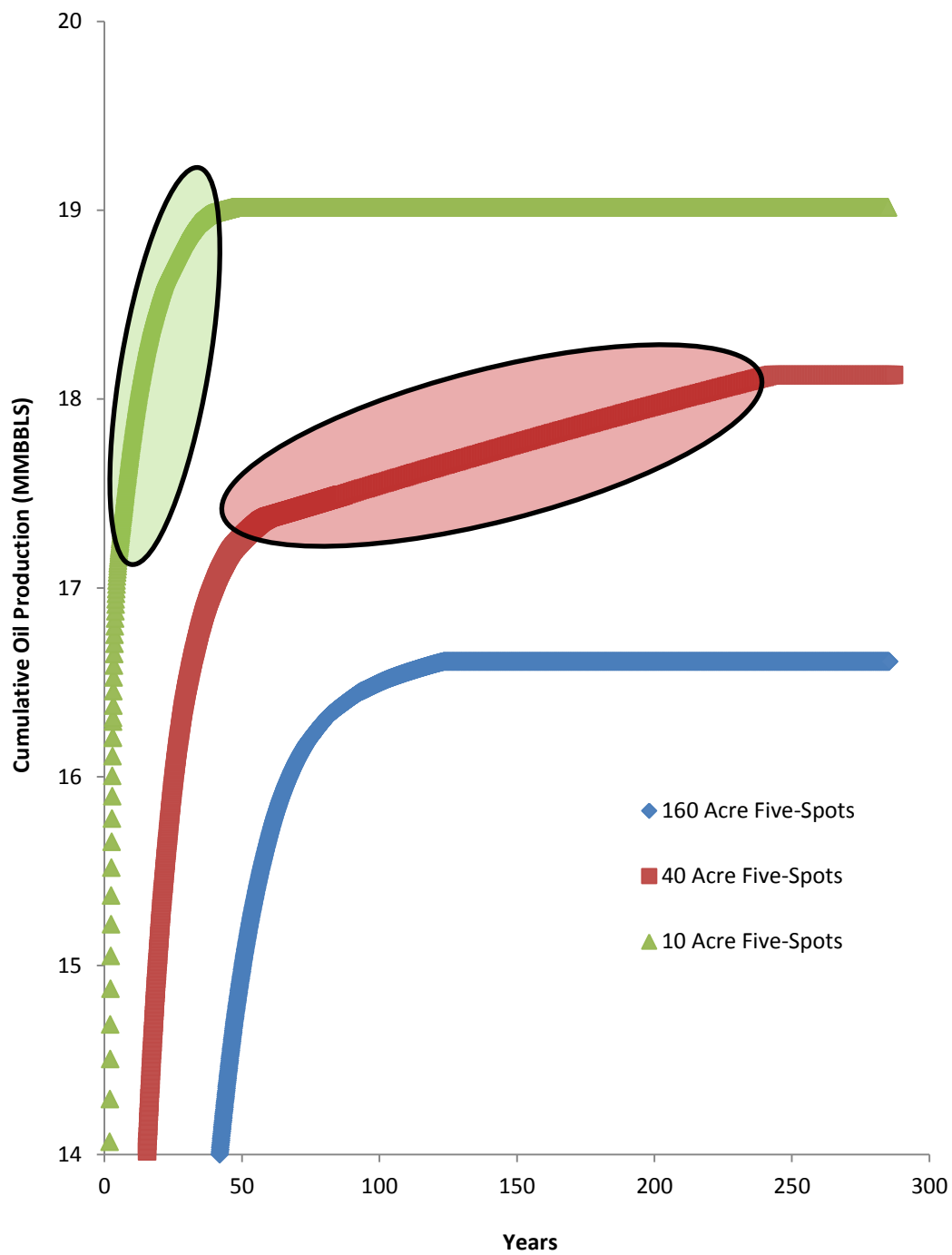


Figure 5.24: Cumulative Oil Production as a Function of Time for a Vertically Discontinuous Reservoir (k_{avg} of Top Two Layers = 1 md, k_{avg} of Bottom Two Layers = 100 md).

To further investigate the impact of well spacing on vertical conformance in layered reservoirs, a two-dimensional vertically discontinuous reservoir model was created (Figure 5.25). As with the aforementioned three-dimensional model, the top two and bottom two layers were assigned average permeabilities of 1 and 100 md, respectively. For the sake of consistency, three development scenarios were also considered in this 2D model. Injection and production wells were placed 1,868 ft, 934 ft, or 467 ft apart.

Simulation results are displayed in Table 5.4. Although decreasing well spacing from 1,868 ft to 934 ft only improved oil recovery by 0.1% OOIP, an additional 2.71% OOIP was recovered through reducing the well separation from 934 to 467 ft. Furthermore, decreasing the distance between wells from 934 to 467 ft was increased recovery time by 3 years. The impact of well spacing on vertical sweep can clearly be observed in Figures 5.26-5.28. While the low permeability layers were unswept regardless of well spacing, the lack of adequate pressure support prevented the high permeability layers from being swept in the widely spaced scenarios.

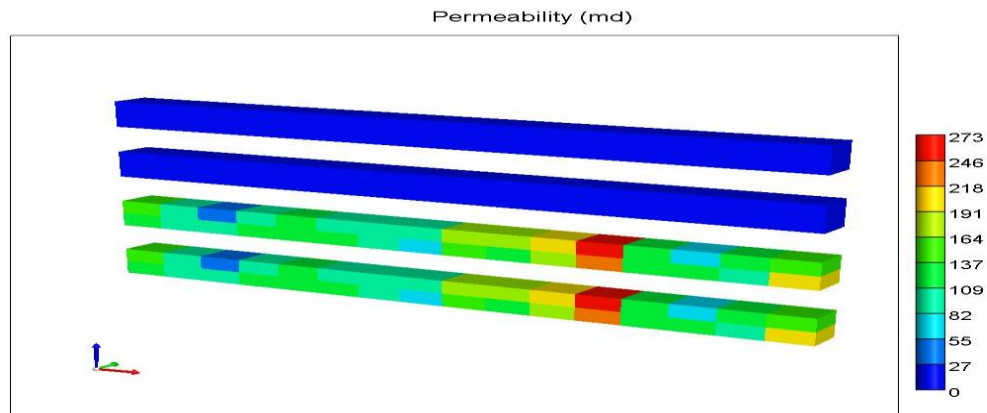


Figure 5.25: Permeability Distribution for a 2D Vertically Discontinuous Reservoir Model (k_{avg} of Top Two Layers = 1 md, k_{avg} of Bottom Two Layers = 100 md).

Well Separation (ft)	Recovery Efficiency (%)	Recovery Time (Years)
1,868	27.54	22
934	27.64	13
467	30.35	16

Table 5.4: Simulation Results for a Two-Dimensional Vertically Discontinuous Reservoir Model Reservoir (k_{avg} of Top Two Layers = 1 md, k_{avg} of Bottom Two Layers = 100 md).

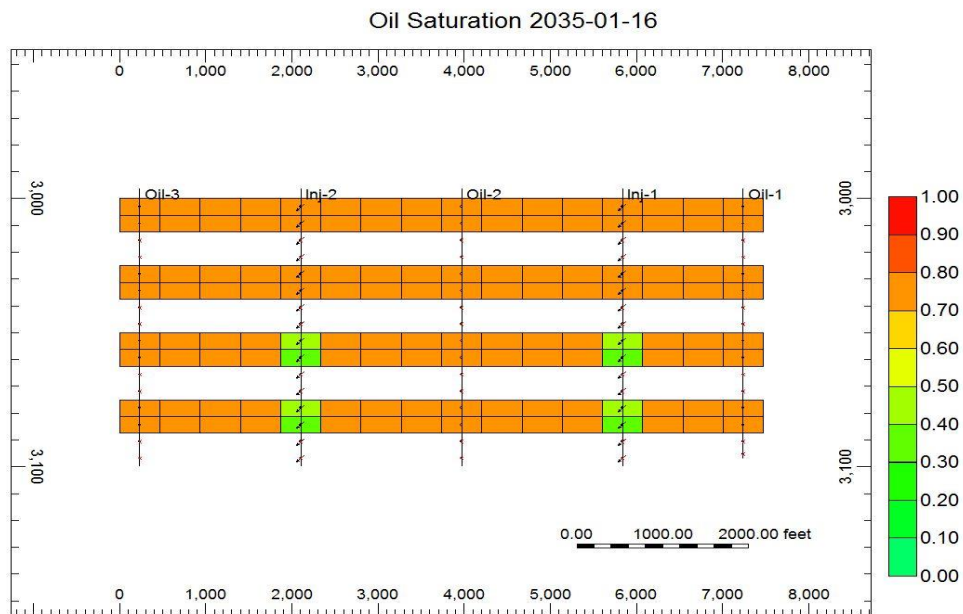


Figure 5.26: Oil Saturation at Simulation Termination for a 2D Vertically Discontinuous Reservoir Model Populated with wells that are 1,868 ft Apart.

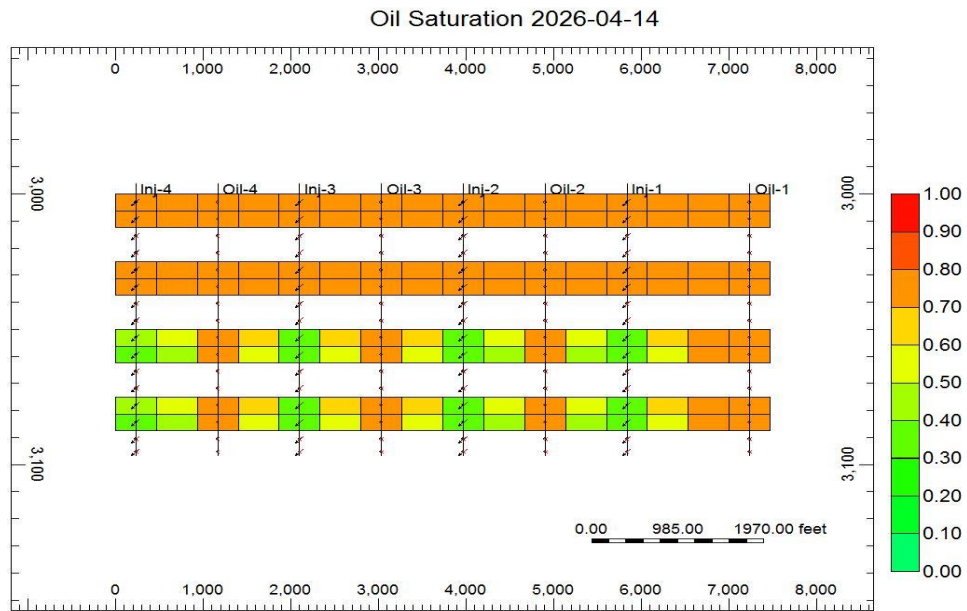


Figure 5.27: Oil Saturation at Simulation Termination for a 2D Vertically Discontinuous Reservoir Model Populated with wells that are 934 ft Apart.

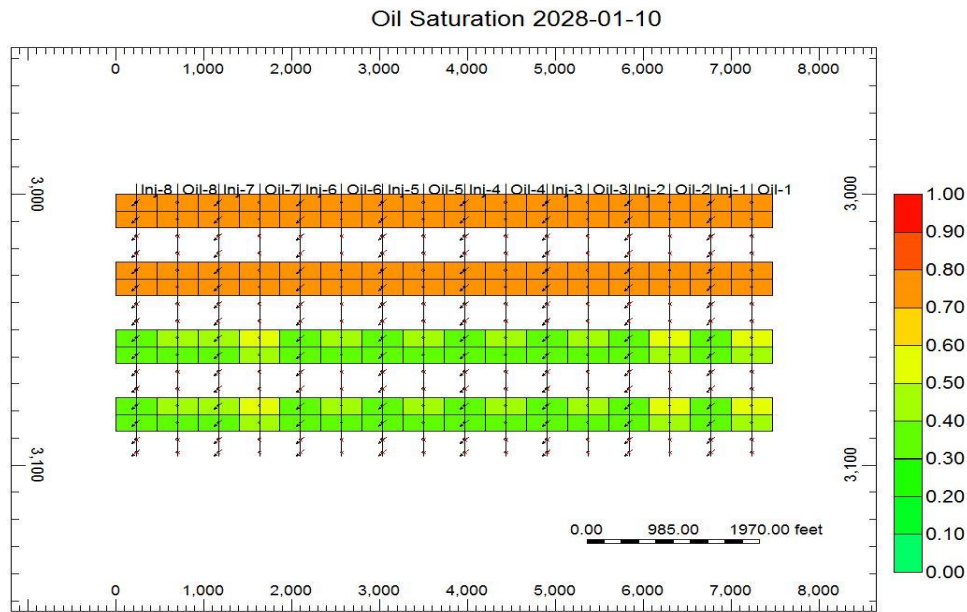


Figure 5.28: Oil Saturation at Simulation Termination for a 2D Vertically Discontinuous Reservoir Model Populated with wells that are 467 ft Apart.

Similar simulations were conducted on several other three-dimensional vertically discontinuous reservoir models. Results indicate that the relationship between waterflood recovery and pattern size is controlled by the variation in average permeability between the different layers. In models where the different layers had comparable average permeability values, pattern size reduction had no influence on ultimate recovery efficiency. Additionally, ultimate waterflood recovery was independent of pattern size in models where all the layers had relatively high permeability values (e.g. 50 md in the top layers, and 100 md in the bottom layers).

One strategy that can be employed, to eliminate the effect of average permeability variations between vertically discontinuous layers, is selective development. Initially, production and injection wells can be perforated only across the high permeability layers. Once the mobile oil in these layers is completely drained, wells can then be completed in the lower permeability layers (or vice versa). Another alternative to prevent permeability variations from dictating vertical sweep would be to designate different wells to different layers based on the average permeabilities of those layers. However, in reservoirs where oil has already been bypassed, ultimate recovery efficiency can be improved by pattern size reduction.

Chapter 6: Summary and Conclusion

6.1 SUMMARY

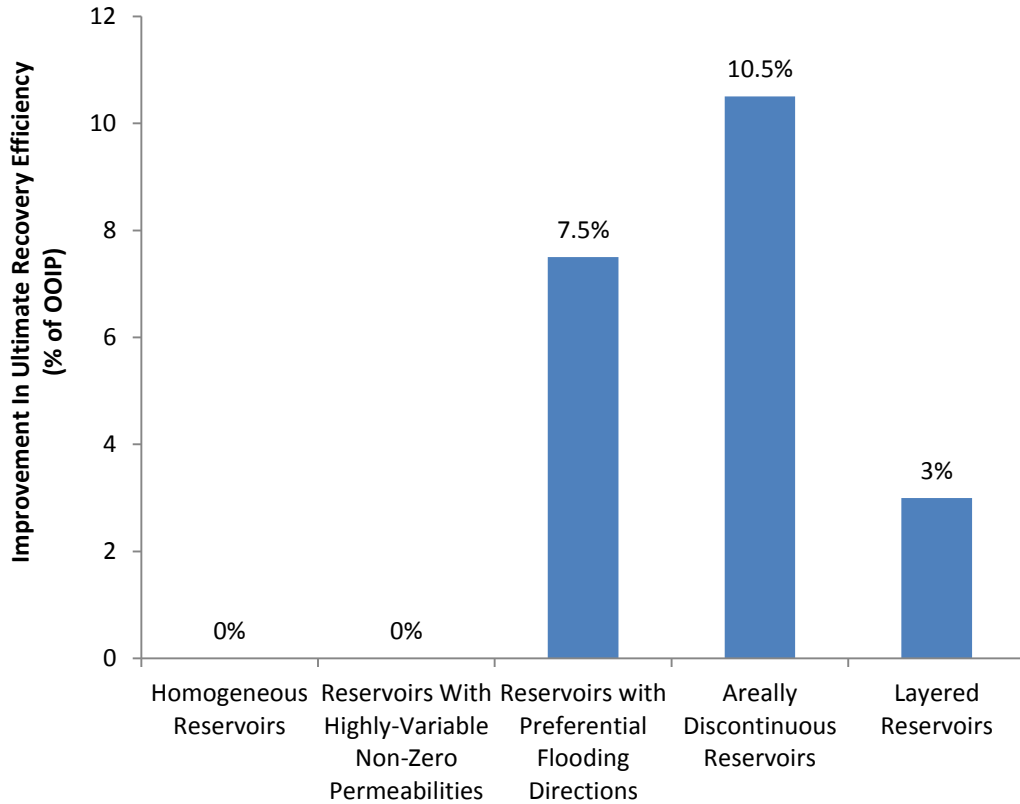


Figure 6.1: The Average Improvement in Ultimate Recovery Efficiency Achieved by Reducing the Pattern Size from 160 to 10 Acre Five-Spots for all the Performed Simulations.

Figure 6.1 was constructed based on averages of all the results completed in this study. This bar chart illustrates the effect of reservoir heterogeneity on infill potential. As shown in Figure 6.1, reducing the pattern size from 160 to 10 acre five-spots did not improve ultimate recovery efficiency in homogeneous reservoirs, or in reservoirs with highly-variable non-zero permeabilities. On the other hand, such reduction in pattern size did enhance ultimate oil recovery in reservoirs with a high degree of permeability

anisotropy, areally discontinuous reservoirs, and layered reservoirs. Simulation results indicate that areally discontinuous reservoir models have the highest infill potential of all the types of models examined in this study. On average, a 10.5% OOIP improvement in ultimate recovery was realized by decreasing the pattern size from 160 to 10 acres in such reservoirs. A significant percentage improvement in ultimate recovery (7.5% OOIP) was also observed in reservoirs with preferential flooding orientations. Additionally, in layered reservoirs, reducing the pattern size from 160 to 10 acres resulted in a 3% OOIP improvement in ultimate recovery. All of these percentages fall within the expected range observed in published field data (1-22% OOIP).

In all the results presented thus far, pattern sizes were reduced through increasing the number of wells penetrating the grid. It is worth noting that another technique was also used to assess the relationship between ultimate waterflood recovery and pattern size. Instead of increasing the number of wells, the dimensions of the grid blocks were altered to achieve the desired pattern size. Using this method, simulation runs were conducted on the same previously presented reservoir models. Results indicated that pattern size did not have the slightest influence on ultimate recovery efficiency. Within each reservoir model, the exact same recovery was achieved regardless of pattern size. Decreasing the grid block sizes did however manage to accelerate oil recovery. These results have similar implications to those obtained from homogeneous models. Unless inter-well reservoir features are altered by pattern size reduction, no impact on ultimate oil recovery will be realized.

Simulation runs were also conducted on infill scenarios. First, reservoir models were developed with 160 acre five-spots. After operating for a period of time, the 160 acre five-spots were converted into 40 acre five-spots through adding wells and converting producers and injectors. This same process was also done to convert 160 acre

five-spots to 10 acre five-spots. Results showed that ultimate waterflood recovery was independent of initial well definition time. Whether wells were defined from day 1 or at a later time, the amount of oil recovered by pattern size reduction would be the same.

The numerical simulation results presented in this study are grid-dependent. The large size of the selected grid blocks has an effect on the obtained ultimate oil recoveries. This effect is more prominent in the 10 acre development scenarios, where all the grid blocks are penetrated by wells. One recommendation for future studies on infill potential would be to apply the concepts presented in this research on finer grid models.

6.2 CONCLUSION

Reservoir heterogeneity is the most important factor to consider when designing any type of waterflood. In cases where pattern flooding is needed, the optimum pattern size required to maximize ultimate oil recovery depends on reservoir geometry and internal characteristics. Widely spaced patterns can result in bypassing significant quantities of oil in areally discontinuous reservoirs, reservoirs with preferential flooding orientations, and vertically discontinuous reservoirs. Numerous studies conducted on published field data advocate for pattern size reduction as a method of improving waterflood recovery in heterogeneous reservoirs. Although these studies depended on decline curve analysis in estimating ultimate recovery, simulations completed in this thesis give merit to their findings.

Homogeneous Reservoirs and Reservoirs with Highly-Variable Non-Zero Permeabilities

In homogeneous reservoir models, recovery efficiency was found to be independent of pattern size. Similarly, pattern size reduction had no influence on the quantity of oil recovered from models with highly-variable non-zero permeabilities.

However, smaller spaced patterns did substantially accelerate oil recovery in these homogeneous and semi-heterogeneous reservoir models.

Reservoirs with Preferential Flooding Directions

In models with a high degree of permeability anisotropy, an inverse relationship was established between pattern size and ultimate recovery efficiency. Uneven waterfront advancement caused by over injection resulted in bypassed oil. The effect of early water breakthrough on ultimate recovery efficiency was less significant on small patterns than on large patterns. While this problem can be avoided by pattern reorientation, it remains one of the reasons that oil recovery is improved by pattern size reduction.

Areal Discontinuous Reservoirs

Simulation results also provided insight on to why the concept of areal reservoir discontinuity appears abundantly in the literature pertaining to pattern size reduction. Depending on the degree of compartmentalization, the gain realized from tighter patterns can be as large as 35.58% OOIP. Unless all reservoir compartments are contacted by both producers and injectors, oil recovery can be improved by decreasing pattern size.

Layered Reservoirs

Infill potential also exists for vertically discontinuous reservoirs. In such reservoirs, vertical sweep is controlled by the contrast in permeability between different layers. Simulation results indicate that pattern size reduction can increase waterflood recovery by improving vertical conformance in layered reservoirs with dissimilar permeabilities.

References

1. W. L. Fisher, *Class Notes for GEO 383R, Reservoir Geology and Advanced Recovery*, The University of Texas at Austin, Fall semester, 2013.
2. C. H. Wu, B. A. Laughlin, M. Jardon, “Infill Drilling Enhances Waterflood Recovery,” *Journal of Petroleum Technology*, vol. 41, no. 10, pp. 1088-1095, Oct. 1989.
3. B.C. Craft and M. Hawkins, *Applied Petroleum Reservoir Engineering*, 2nd ed. New Jersey: Prentice Hall, Inc., 1991.
4. K. E. Gulick and W. D. McCain Jr., “Waterflooding Heterogeneous Reservoirs: An Overview of Industry Experiences and Practices,” Paper SPE 40044 presented at the SPE International Petroleum Conference and Exhibition, Villahermosa, Mexico, Mar. 3-5, 1998.
5. L. P. Dake, *The Practice of Reservoir Engineering*, revised ed. Oxford: Elsevier, 2001.
6. P. B. Gadde and M. M. Sharma, “Growing Injection Well Fractures and Their Impact on Waterflood Performance,” Paper SPE 71614 presented at the SPE Annual Technical Conference and Exhibition, New Orleans, Louisiana, 30 Sept. – 3 Oct., 2001.
7. W. C. Lyons, *Standard Handbook of Petroleum & Natural Gas Engineering*, vol. 2, Houston: Gulf Publishing Company, 1996.
8. W. R. Emmett, K. W. Beaver, J. A. McCaleb, “Little Buffalo Basin Tensleep Heterogeneity – Its Influence on Drilling and Secondary Recovery,” *Journal of Petroleum Technology*, vol. 23, no. 02, pp. 161-168, Feb. 1971.

9. V. J. Driscoll, "Recovery Optimization Through Infill Drilling – Concepts, Analysis, and Field Results," Paper SPE 4977 presented at the 49th annual Fall Meeting of the SPE of AIME, Houston, Texas, Oct. 6-9, 1974.
10. A. F. van Everdingen, H. S. Kriss, "A Proposal to Improve Recovery Efficiency," *Journal of Petroleum Technology*, vol. 32, no. 07, pp. 1164-1168, May 1980.
11. L. R. Kern, "Effect of Spacing on Waterflood Recovery Efficiency," Paper SPE 10538, 1981.
12. A. H. Barber Jr., C. J. George, L. H. Stiles, B. B. Thompson, "Infill Drilling to Increase Reserves – Actual Experience in Nine Fields in Texas, Oklahoma, and Illinois," *Journal of Petroleum Technology*, vol. 35, no. 08, pp. 1530-1538, May 1983.
13. M. L. Mahmoud, "Infill Drilling Enhances Oil Recovery in Egypt's First Waterflood Field," Paper SPE 15762 presented at the Fifth SPE Middle East Oil Show, Manama, Bahrain, Mar. 7-10, 1987.
14. M. A. Lemen, T. C. Burlas, L. M. Roe, "Waterflood Pattern Realignment at the McElroy Field: Section 205 Case History" Paper SPE 20120 presented at the Permian Basin Oil and Gas Recovery Conference, Midland, Texas, Mar. 8-9, 1990.
15. G. W. L. Kwan, "Correlating Waterflood Ultimate Recovery with Controllable Field Operating Variable in Prudhoe Bay," Paper SPE 24647 presented at the 67th Annual Technical Conference and Exhibition in Washington, D.C., Oct. 4-7, 1992.
16. D. J. Suttles and G. W. L. Kwan, "Pattern Size Reduction: A Reservoir Management Tool for Prudhoe Bay Waterfloods," Paper SPE 26117 presented at the Western Regional Meeting, Anchorage, Alaska, May 26-28, 1993.

17. L. H. Stiles, "Optimizing Waterflood Recovery in a Mature Waterflood, The Fullerton Clearfork Unit," Paper SPE 6198 presented at the 51st Annual Fall Technical Conference and Exhibition, New Orleans, Louisiana, Oct. 3-6, 1976.
18. W. L. Maguson, J. D. Knowles, "Denver Unit 10-Acre Infill Pilot Test and Residual Oil Testing," Paper SPE 6385 presented at Permian Basin Oil and Gas Recovery Conference, Midland, Texas, Mar. 10-11, 1977.
19. J. E. Thomas and V. J. Driscoll, "A Modeling Approach for Optimizing Waterflood Performance, Slaughter Field Chickenwire Pattern," *Journal of Petroleum Technology*, vol. 25, no. 07, pp. 757-763, July 1973.
20. Shell Oil Co., "Application for Waterflood Response Allowable for Wasson Denver Unit," *Hearing Testimony before Texas Railroad Commission, Docket 8-A-61677*, Mar. 21, 1972.
21. W. D. McCain Jr., *The Properties of Petroleum Fluids*, 2nd ed. Tulsa: Penn Well Corporation, 1990.
22. J. W. Jennings, S. C. Ruppel, W. B. Ward, "Geostatistical Analysis of Permeability Data and Modeling of Fluid-Flow Effects in Carbonate Outcrops," *SPE Reservoir Evaluation and Engineering*, vol. 3, no. 4, pp. 292-303, Aug. 2000.
23. S. Bryant, *Class notes for PGE 381L, Advanced Petrophysics*, The University of Texas at Austin, Fall semester, 2012.